TLR9 ligation in pancreatic stellate cells promotes tumorigenesis

Constantinos P. Zambirinis,[1] Elliot Levie,[1] Susanna Nguy,[1] Antonina Avanzi,[1] Rocky Barilla,[1] Yijie Xu,[1] Lena Seifert,[1] Donnele Daley,[1] Stephanie H. Greco,[1] Michael Deutsch,[1] Saikiran Jonnadula,[1] Alejandro Torres-Hernandez,[1] Daniel Tippens,[1] Smruti Pushalkar,[5] Andrew Eisenthal,[1] Deepak Saxena,[5] Jiyoung Ahn,[2] Cristina Hajdu,[3] Dannielle D. Engle,[6] David Tuveson,[6] and George Miller[1,4]

[1]Department of Surgery, [2]Department of Population Health, [3]Department of Pathology, and [4]Department of Cell Biology, New York University School of Medicine, New York, NY 10016
[5]New York University College of Dentistry, New York, NY 10016
[6]Cold Spring Harbor Laboratories, Cold Spring Harbor, NY 11724

Modulation of Toll-like receptor (TLR) signaling can have protective or protumorigenic effects on oncogenesis depending on the cancer subtype and on specific inflammatory elements within the tumor milieu. We found that TLR9 is widely expressed early during the course of pancreatic transformation and that TLR9 ligands are ubiquitous within the tumor microenvironment. TLR9 ligation markedly accelerates oncogenesis, whereas TLR9 deletion is protective. We show that TLR9 activation has distinct effects on the epithelial, inflammatory, and fibrogenic cellular subsets in pancreatic carcinoma and plays a central role in cross talk between these compartments. Specifically, TLR9 activation can induce proinflammatory signaling in transformed epithelial cells, but does not elicit oncogene expression or cancer cell proliferation. Conversely, TLR9 ligation induces pancreatic stellate cells (PSCs) to become fibrogenic and secrete chemokines that promote epithelial cell proliferation. TLR9-activated PSCs mediate their protumorigenic effects on the epithelial compartment via CCL11. Additionally, TLR9 has immune-suppressive effects in the tumor microenvironment (TME) via induction of regulatory T cell recruitment and myeloid-derived suppressor cell proliferation. Collectively, our work shows that TLR9 has protumorigenic effects in pancreatic carcinoma which are distinct from its influence in extrapancreatic malignancies and from the mechanistic effects of other TLRs on pancreatic oncogenesis.

Pancreatic ductal adenocarcinoma (PDAC) is the fourth most lethal cancer in the U.S., with a 5-yr mortality rate exceeding 95% (American Cancer Society, 2013). PDAC is an inflammation-driven cancer. Chronic pancreatitis is the most well-established risk factor for PDAC, with these patients carrying an ~15-fold increased risk of PDAC development (Yadav and Lowenfels, 2013). Patients with hereditary autoimmune pancreatitis have an estimated lifetime risk for PDAC development of 40–70% (Bartsch et al., 2012). Notably, pancreatic inflammation not only accompanies PDAC but is necessary for tumor progression, as oncogenic mutation alone in the absence of chronic inflammation is an insufficient driving force for tumorigenesis (Guerra et al., 2007).

Toll-like receptors (TLRs) are pattern-recognition receptors that recognize conserved motifs found in microbes, called pathogen-associated molecular patterns (PAMPs), as well as byproducts of cellular injury and sterile inflammation,

called damage-associated molecular patterns (DAMPs). Upon ligand binding, TLRs homodimerize or heterodimerize, resulting in the recruitment of adaptor molecules (Takeda and Akira, 2007). All TLRs, with the exception of TLR3, transduce their signal through the MYD88 adaptor, whereas TLR3 recruits TRIF instead of MYD88. TLR4 can associate with both MYD88 and TRIF. Downstream signal transduction results in activation of diverse pathways, the most notable being MAP Kinase and NF-κB (Takeuchi and Akira, 2010).

We have previously shown that activation of TLR signaling can have divergent effects on pancreatic tumorigenesis. For example, signaling via TLR4, TLR7, or TRIF accelerates PDAC development by fueling intrapancreatic inflammation (Ochi et al., 2012a,b). However, rather than protecting against carcinoma, blockade of MyD88 surprisingly accelerates tumorigenesis by promoting DC induction of proinflammatory Th2-deviated CD4+ T cells (Ochi et al., 2012b). In this study, we show that TLR9 is expressed in dysplastic and neoplastic pancreata and its activation early in the course

The Rockefeller University Press $30.00
J. Exp. Med. 2015 Vol. 212 No. 12   2077–2094
www.jem.org/cgi/doi/10.1084/jem.20142162

2077

of PDAC development has robust protumorigenic effects. Further, TLR9 ablation affords tumor protection and improves survival in a murine model of pancreatic carcinogenesis. We demonstrate that TLR9 activation has direct effects on transformed pancreatic epithelial cells, as well as on the proliferation of myeloid-derived suppressor cells (MDSCs). Further, TLR9 stimulation reprograms pancreatic stellate cells (PSCs) into a central hub emanating diverse signals to promote tumor growth, fibroinflammation, and recruitment of regulatory T cells.

RESULTS

TLR9 is up-regulated in PDACs

To determine the relevance of TLR9 to pancreatic oncogenesis, we investigated its expression in p48^{Cre};LsL-Kras^{G12D} (KC) mice. We found that TLR9 is widely expressed in the pancreata of 3-mo-old KC mice (Fig. 1 A). To analyze the specific cellular subsets within the TME that express TLR9, we performed flow cytometry on the pancreata of 3- and 6-mo-old KC mice and found that TLR9 is expressed on innate inflammatory cells, including DCs (CD45$^+$CD11c$^+$ MHCII^{high}), granulocytes (CD45$^+$CD11c$^-$Ly6G$^+$), and macrophages (CD45$^+$CD11c$^-$Ly6G$^-$Ly6C$^+$CD11b$^+$F4/80$^+$; Fig. 1 B). TLR9 was also expressed on CD45$^-$CD34$^-$CD133$^+$ pancreatic ductal epithelial cells (Ochi et al., 2012a) and PDGFR-α$^+$ cancer-associated fibroblasts (CAFs; Erez et al., 2010; Fig. 1 C). Similarly, human PDAC sections stained diffusely for TLR9 in the epithelial and stromal compartments, whereas normal pancreas did not (Fig. 1 D). We also found high levels of high-mobility group protein B1 (HMGB1) in human PDACs (Fig. 1 E), suggesting the presence of endogenous ligands that can bind TLR9 or TLR4 (Yanai et al., 2012; Hirata et al., 2013).

TLR9 ligation accelerates pancreatic oncogenesis

To examine whether TLR9 ligation modulates PDAC progression, we treated KC mice with TLR9 ligand ODN1826 (CpG). We found that CpG accelerated oncogenesis in 14-wk-old KC mice by pancreas weight (Fig. 2 A). Further, CpG treatment was associated with precocious development of advanced PanIN lesions and foci of invasive cancer, accelerated fibrosis, and a rich peritumoral inflammatory infiltrate (Fig. 2 B). CpG similarly accelerated oncogenesis in 22-wk-old KC mice (Fig. 2, C and D).

Analysis of protein expression in pancreas lysates revealed higher activity of proinflammatory pathways in pancreata of CpG-treated KC mice as indicated by increased phosphorylation of STAT3, NF-κB, and MAP kinase signaling intermediates, which are associated with accelerated pancreatic tumorigenesis (Fig. 2 E; Surh et al., 2010; Ochi et al., 2012a). Similarly, TLR9 ligation induced elevated expression of c-Myc, p53, p27, Cyclin D1, Cyclin B1, Bcl-X$_L$, and Bcl-2, suggesting that TLR9 activation results in up-regulated expression of numerous oncogenic targets (Fig. 2 E). Notably, in vivo administration of CpG for as short a duration as

4 d was sufficient to induce marked up-regulation of Bcl-2 and Bcl-X$_L$ in KC mice, whereas it had minimal effects in WT pancreata (Fig. 2 F).

In addition to tumor microenvironmental DAMPs, a potential source of TLR9 ligands in invasive or preinvasive PDAC may be gut or systemic microbiota (Zambirinis et al., 2014). We tested whether luminal or systemic bacteria can access the pancreas by administering fluorescently labeled *S. mutans* to mice via oral gavage or i.p. injection. We found that luminal as well as peritoneal bacteria can indeed access the pancreas (Fig. 3 A). Similarly, fluorescently-labeled CpG was taken up avidly by pancreatic APC after administration by oral gavage (Fig. 3 B). Moreover, administration of CpG via oral gavage accelerated disease progression, suggesting that luminal PAMPs specific for TLR9 can promote pancreatic oncogenesis (Fig. 3 C).

TLR9 deletion is protective against pancreatic oncogenesis

To determine whether TLR9 is necessary for pancreatic oncogenesis, we crossed TLR9$^{-/-}$ mice with KC mice to generate p48$^{+/Cre}$;LsL-Kras$^{G12D/+}$;TLR9$^{-/-}$ (KC;TLR9$^{-/-}$) mice. Pancreata of KC;TLR9$^{-/-}$ animals weighed significantly less than pancreata of age-matched KC;TLR9$^{+/+}$ mice (Fig. 4 A). KC;TLR9$^{-/-}$ animals also exhibited less morphological transformation and had a decreased fraction of proliferating pancreatic ductal epithelial cells compared with KC;TLR9$^{+/+}$ pancreata (Fig. 4 B). Kaplan-Meier survival analysis further showed a substantial protective effect of TLR9 deletion (Fig. 4 C). Collectively, these data suggest that TLR9 is necessary for pancreatic oncogenesis to proceed at its expected rate in mice with a driving oncogenic *Kras* mutation.

TLR9 ligation activates proinflammatory pathways in transformed epithelial cells but does not have direct oncogenic effects

Because we found that TLR9 is up-regulated on fibrogenic, inflammatory, and epithelial cells (Fig. 1, A–C), we tested its tumor-modulating effects in each compartment. We first examined the effects of TLR9 ligation on the human PDAC cell lines AsPC1 and BxPC3, which express mutant and WT *Kras*, respectively (Deer et al., 2010). Each cell line expressed TLR9 (Fig. 5 A), although AsPC1 exhibited more than fivefold higher expression by qPCR analysis (Fig. 5 B). Stimulation with CpG increased NF-κB phosphorylation in AsPC1 but not in BxPC3 cells; however, both cell lines activated MAP kinase signaling in response to TLR9 ligation (Fig. 5 C). BxPC3 cells up-regulated the secretion of IL-6 after stimulation with CpG (Fig. 5 D) and both cell lines increased their secretion of IL-8 (Fig. 5 E). Other tumor-modulatory cytokines assessed (TNF, IL-10, and IL-1β) were not secreted at detectable levels. Notably, TLR9 ligation did not affect the proliferation rate of either AsPC1 or BxPC3 (Fig. 5 F), nor did it cause marked alterations in expression levels of oncogenic or cell cycle regulatory proteins associated with CpG-induced acceler-
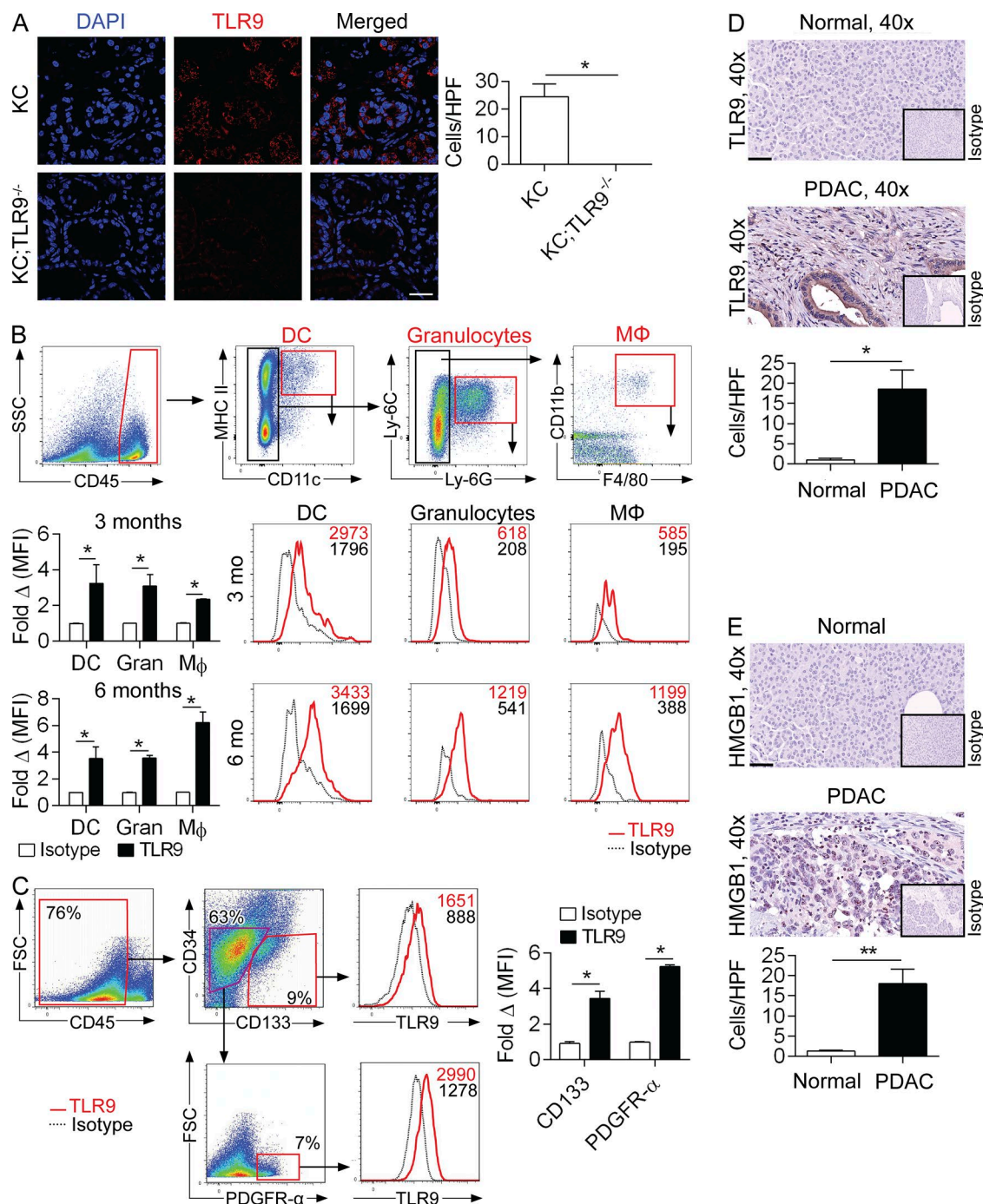
Figure 1. **TLR9 is up–regulated during pancreatic oncogenesis in epithelial, inflammatory, and stromal cells.** (A) Frozen sections from pancreata of 3-mo-old KC and KC;TLR9$^{-/-}$ mice were stained for DAPI and TLR9 and visualized on a confocal microscope (63×; bar = 30 µm). Results were quantified based on 10 HPFs per slide. (B) 3- and 6-mo-old KC mice were analyzed by flow cytometry for pancreatic TLR9 expression on DCs, granulocytes, and macrophages. Mean fluorescence intensity (MFI) is indicated compared with respective isotype controls. Representative data and summary statistics from three mice per data point are shown. (C) 3-mo-old KC mice were analyzed by flow cytometry for pancreatic TLR9 expression on epithelial cells (CD45$^-$CD34$^-$CD133$^+$) and cancer-associated fibroblasts (CD45$^-$CD34$^-$CD133$^-$PDGFR-α$^+$). Representative data and summary statistics from three mice per data point are shown. Mouse experiments were repeated more than five times with similar results. (D) TLR9 immunohistochemistry compared with isotype control was performed on normal human pancreata and pancreata from patients with PDAC (40×; bar = 60 µm). Representative images and quantitative data from four patients per group are shown. (E) Human PDAC and normal human pancreas specimens were stained using a mAb directed against HMGB1 (40×; bar = 60 µm). Representative images and quantitative data from four patients per group are shown ($*$, P < 0.05; $**$, P < 0.01 using the Student's t test).
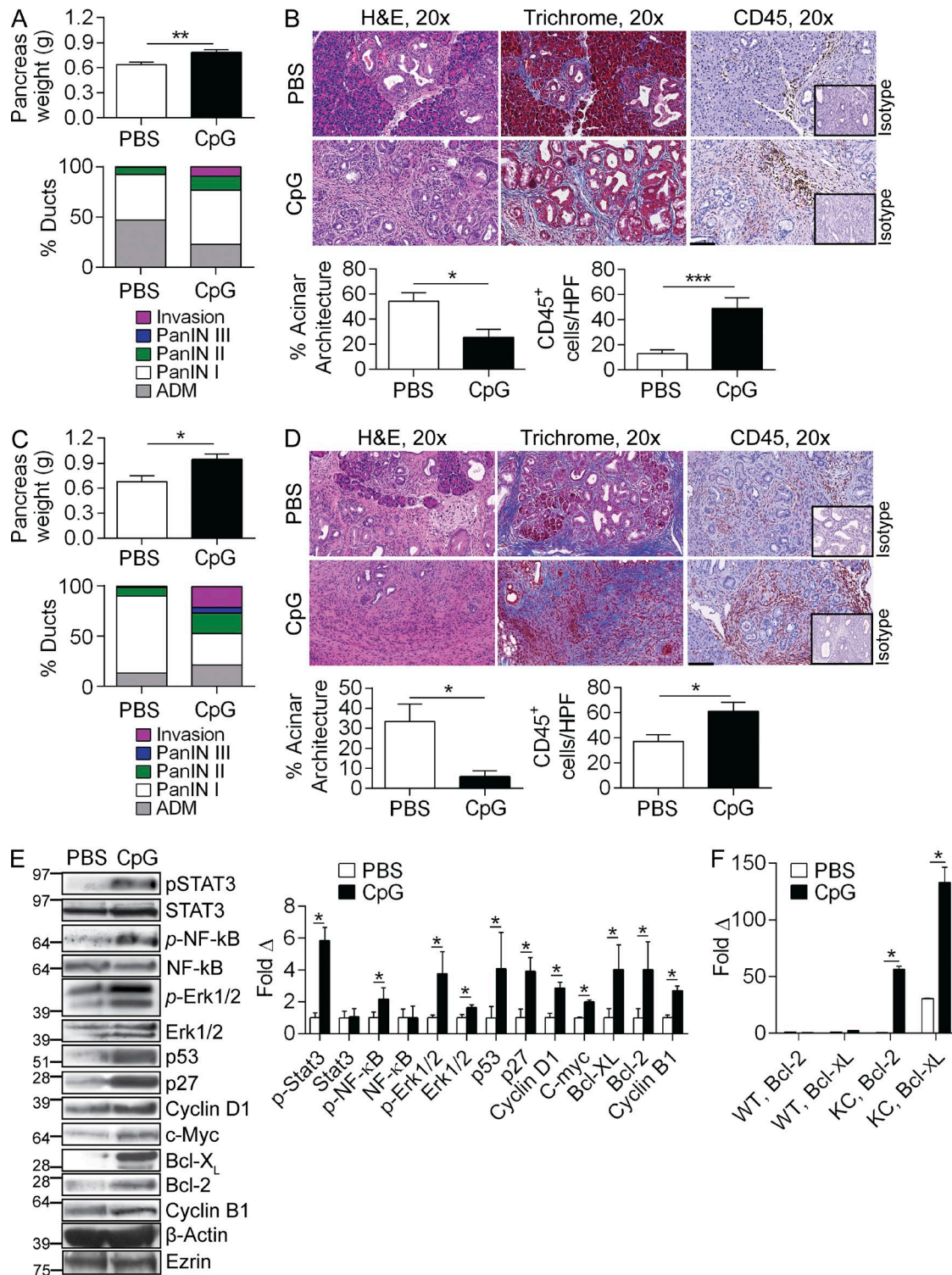
Figure 2. **TLR9 activation accelerates pancreatic oncogenesis.** (A) 10-wk-old KC mice were administered CpG or PBS thrice weekly by i.p. injection for 4 wk. Pancreata were harvested and weighed (*n* = 9/group). (B) Pancreatic sections were stained with H&E, Trichrome, and IHC was performed using an anti-CD45 mAb compared with isotype control. The fraction of pancreatic ducts exhibiting normal morphology, acinoductal metaplasia (ADM), various grades of PanIN, or foci of invasive carcinoma were quantified. Similarly, the fraction of preserved acinar area and the number of CD45+ cells per HPF were quantified (20×; bar = 100 µm). (C and D) Similarly, cohorts of 10-wk-old KC were serially administered CpG or PBS for 12 wk (*n* = 5/group). Pancreata were weighed, stained with H&E, trichrome, and CD45. Morphological transformation and inflammatory cell infiltration were quantified as above. (E) Pancreata

ated tumorigenesis (Fig. 5 G). Similarly, gene expression profiling did not reveal significant changes in the expression of oncogenic genes after TLR9 activation in AsPC1 or BxPC3 cells (Fig. 5 H).

To further investigate the direct effects of TLR9 ligation on transformed epithelial cells, we performed parallel experiments in murine pancreatic cancer cells using both Pdx^{Cre};LsL-Kras^{G12D};p53^{R172H} (KPC) mouse–derived RoBa cells, and the Pan02 cell line, which expresses WT *Kras*. Both RoBa and Pan02 cells expressed TLR9 (Fig. 6 A). Stimulation with CpG resulted in activation of NF-κB, Akt, and Erk1/2 in RoBa cells but not in Pan02 cells (Fig. 6 B). However, no changes were observed in the expression of oncogenic or tumor-suppressor proteins or in cellular proliferation upon TLR9 ligation (Fig. 6, C and D). Similarly, CpG treatment did not enhance the proliferation of *Kras*-transformed pancreatic ductal epithelial cells (Kras^{G12D}-PDEC) harvested from KC mice (Fig. 6 E). Further, genetic deletion of TLR9 did not mitigate the proliferative capacity of Kras^{G12D}-PDEC (Fig. 6 F). These findings suggest that TLR9 ligation may activate proinflammatory pathways in human and murine pancreatic cancer cells but this is not sufficient to promote increased proliferation or oncogenic changes.

We postulated that TLR9 signaling induces protumorigenic effects in the extraepithelial compartment. To test this, we orthotopically implanted KPC-derived FC1242 cells into the pancreata of WT and TLR9$^{-/-}$ mice. TLR9 deletion in the noncancer cells was markedly protective (Fig. 6 G). Similarly, Kras^{G12D}-PDEC formed tumors at slower rates in TLR9$^{-/-}$ mice compared with WT (Fig. 6 H). Conversely, consistent with our in vitro data, TLR9$^{-/-}$;Kras^{G12D}-PDEC did not have diminished growth in vivo compared with TLR9$^{+/+}$;Kras^{G12D}-PDEC (unpublished data). To investigate whether the protection afforded by deletion of TLR9 in the extraepithelial compartment is specific to the pancreatic tumor microenvironment, we implanted FC1242 cells subcutaneously in WT and TLR9$^{-/-}$ mice. However, deletion of TLR9 was not protective against PDAC growth outside of the pancreatic milieu (Fig. 6 I).

TLR9 activation in PSCs sustains a proinflammatory tumor microenvironment via CCL11

Consistent with TLR9 expression on PDGFR-α$^+$ CAFs in vivo (Fig. 1 C), we found that TLR9 is robustly expressed on PSCs in culture using immunofluorescence imaging and flow cytometry (Fig. 7, A and B). Further, PSCs readily responded to TLR9 stimulation by activating MAP kinase and NF-κB

signaling pathways (Fig. 7 C). TLR9 stimulation of PSCs also resulted in up-regulated expression of cytokines (Il1α, Il10, and Tnfα), chemokines (Ccl3, Ccl11, and Ccl12), and regulators of extracellular matrix remodeling (Mmp3, Mmp9, Mmp13, and Timp4; Fig. 7 D). Western blotting confirmed up-regulation of MMP3 and TIMP4 after CpG treatment of PSCs (Fig. 7 E). Because several of the inflammatory mediators overexpressed by PSCs in response to TLR9 ligation (CCL12, IL-1α, and TNF) have established protumorigenic roles in PDAC (Gukovsky et al., 2013; Zheng et al., 2013), we directed further investigations on CCL3 and CCL11, which have not been studied in the context of pancreatic oncogenesis. Using PSCs derived from either WT or TLR9$^{-/-}$ mice, we confirmed that CCL3 and CCL11 are up-regulated upon CpG stimulation in a TLR9-specific manner at the mRNA and protein levels (Fig. 7, F and G).

PSC interface with transformed pancreatic epithelial cells promotes tumor progression (Vonlaufen et al., 2008). We postulated that TLR9 ligation on PSCs enhances their cross talk with the epithelial compartment. To test this, we transplanted WT mice orthotopically with an intrapancreatic injection of KPC-derived FC1242 cells alone (10^5), FC1242 cells + WT PSCs (1:1 ratio), or FC1242 + TLR9$^{-/-}$ PSCs. As anticipated, co-administration of WT PSCs accelerated tumor growth. However, TLR9$^{-/-}$ PSCs were ineffectual at enhancing tumor growth (Fig. 7 H). These data imply that TLR9 signaling in PSCs is necessary in their capacity to support tumor progression. We confirmed that in vivo administration of WT PSCs resulted in higher TLR9 expression in CAFs in orthotopic tumors compared with administration of TLR9$^{-/-}$ PSCs (Fig. 7 I). To further investigate the relationship between TLR9 signaling in PSC and PDAC growth, we cultured KPC-derived RoBa cells or the Pan02 cell line with conditioned media derived from CpG-treated PSCs or controls. We found that conditioned media from CpG-treated PSCs enhanced the growth potential of cancer cells compared with conditioned media from untreated PSCs; conversely, conditioned media derived from TLR9$^{-/-}$ PSCs stimulated with CpG had no effect on cancer cell growth (Fig. 7, J and K).

We next investigated the mechanism of induction of PDAC growth by TLR9-activated PSCs. To examine whether PDAC cells are capable of responding to CCL3 and CCL11, we tested tumor cell expression of their respective chemokine receptors, CCR5 and CCR3. Pancreatic cancer cells expressed CCR3 but not CCR5, suggesting that they may respond directly to CCL11 stimulation (Fig. 8 A). To test this, we treated KPC-derived RoBa cells and Pan02

from 10-wk-old KC mice treated with PBS or CpG for 4 wk were tested for expression of inflammatory signaling intermediates, cell cycle regulators, and oncogenic proteins by Western blotting. β-actin and Ezrin were used as loading controls. Representative data and averages of triplicates based on band intensity relative to respective loading controls are shown. (F) 10-wk-old WT and KC mice were administered CpG or PBS for 4 d and tested for expression of Bcl-2 and Bcl-X$_L$ by PCR. This experiment was performed in quadruplicate and repeated twice with similar results (n = 3/group; *, P < 0.05; ***, P < 0.001 using the Student's t test).
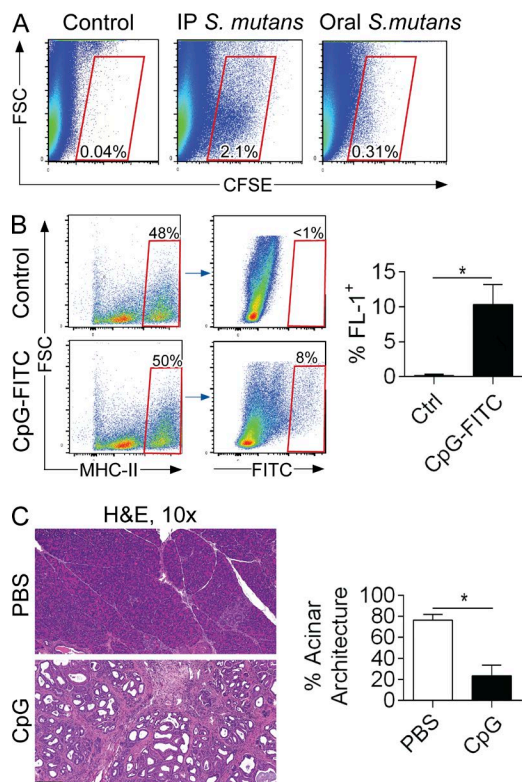
Figure 3.   **Luminal TLR9 ligands can accelerate pancreatic oncogenesis.** (A) 8-wk-old WT mice were administered CFSE-labeled *S. mutans* (10[8]) by the i.p. or oral gavage route. Pancreata were harvested at 6 h and examined by flow cytometry for CFSE^{+} cells compared with PBS-treated control mice. Representative data are shown. The experiment was performed on three separate occasions using up to five mice per group. (B) Cerulein-treated WT mice were administered FITC-labeled CpG (25 µg) by oral gavage. Pancreata were harvested at 6 h, and MHCII^{+} cells were gated and tested for FITC. Representative and quantitative data are shown (*n* = 4/ group). (C) 6-wk-old KC mice were administered CpG or PBS thrice weekly by oral gavage for 5 wk (*n* = 5/group). Pancreata were stained with H&E and the fraction of preserved acinar area was calculated (10×; bar = 200 µm; *, P < 0.05 using the Student's *t* test).

Figure 4.   **TLR9 deletion is protective against pancreatic tumorigenesis.** (A) 6-mo-old KC and KC;TLR9$^{-/-}$ mice were sacrificed and their pancreata were harvested and weighed (*n* = 5/group). (B) H&E stained sections were assessed histologically and the fraction of nontransformed acini was quantified (10×; bar = 200 µm). Tumor proliferation was assessed by Ki67 staining (40×; bar = 60 µm; *, P < 0.05; **, P < 0.01 using the Student's *t* test). (C) Cohorts of KC (*n* = 29) and KC;TLR9$^{-/-}$ (*n* = 46) mice were observed for 2 yr in a Kaplan-Meier survival analysis (P = 0.004 using the Gehan-Breslow-Wilcoxon Test).

cells with recombinant CCL11. As predicted, CCL11 increased their respective proliferation rates in a dose-dependent manner (Fig. 8, B and C). Similarly, CCL11 modestly increased the proliferative rate of Kras^{G12D}-PDEC (Fig. 8 D). Further, recombinant CCL11 or conditioned media of CpG-treated PSCs each induced increased p27 and Bcl-2 expression in tumor cells (Fig. 8 E). To definitively test whether PSC-derived CCL11 is a critical mediator in the tumor-promoting effects of TLR9 ligation in PDAC, we performed blocking experiments in vitro and in vivo. We cultured tumor cells with conditioned media derived from untreated or CpG-treated PSCs in the presence or absence of an α–CCL11–neutralizing mAb. CCL11 blockade abrogated the proproliferative effect of conditioned media derived from CpG-stimulated PSCs (Fig. 8 F). To examine this dependence in vivo, we treated KC mice with PBS or CpG
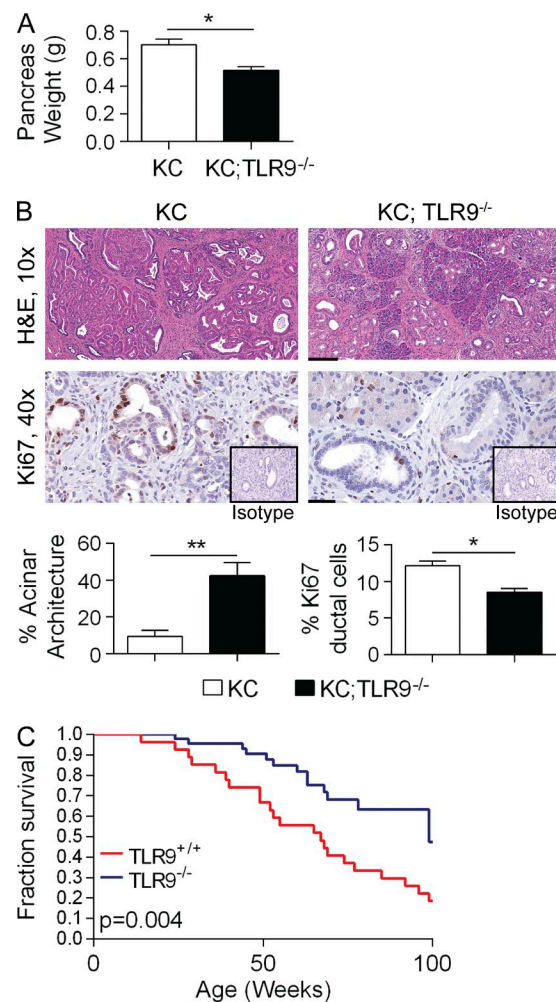
alone, or in combination with a neutralizing α–CCL11 mAb. As predicted, CCL11 blockade protected KC mice from the protumorigenic effects of TLR9 ligation and reduced epithelial cell proliferation (Fig. 8 G). Similarly, whereas TLR9 ligation accelerated the growth of tumors in KPC mice, CCL11 blockade was protective (Fig. 8 H). CCL11 blockade also significantly mitigated the growth of orthotopically implanted KPC-derived FC1242 tumors (Fig. 8 I). Further, KC;TLR9$^{-/-}$ mice, which we showed were protected from pancreatic oncogenesis (Fig. 3) had decreased intrapancreatic levels of CCL11, confirming that TLR9 has a key role in the production of CCL11 in vivo (Fig. 8 J).
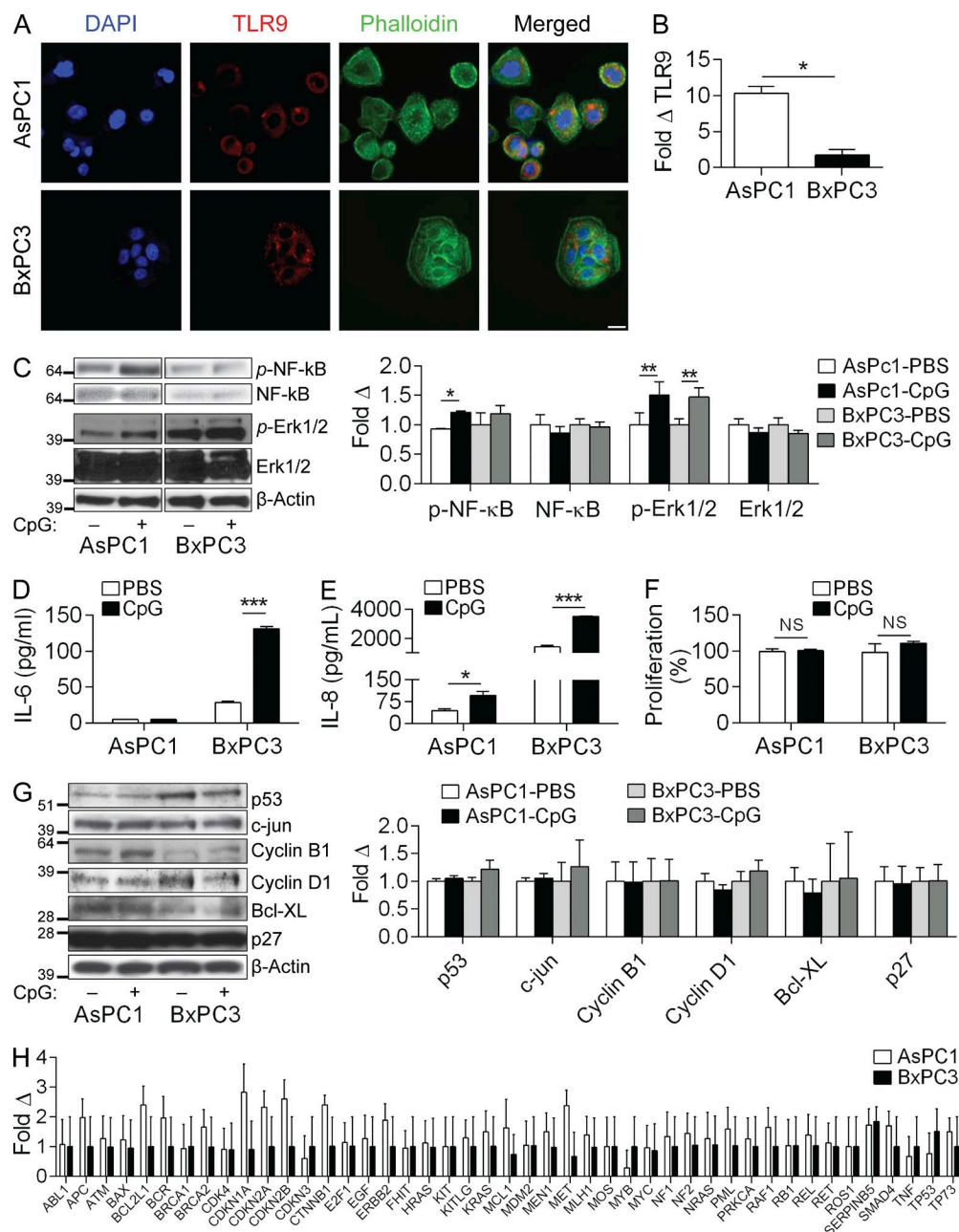
Figure 5. **TLR9 ligation in human pancreatic cancer cells can induce inflammatory signaling but does not elicit oncogenic changes.** (A) AsPC1 and BxPC3 cells were seeded on glass coverslips, stained with anti–TLR9 antibody, and imaged on a confocal microscope (40×; bar = 40 µm). (B) The relative levels of Tlr9 expression in AsPC1 and BxPC3 cells were quantified by qRT-PCR (normalized to β-actin). (C) AsPC1 and BxPC3 cells were either unstimulated or stimulated with CpG (1 µM) for 10 min and Western blotting was performed on whole-cell lysates for NF-κB and MAP kinase signaling intermediates. Results were quantified based on triplicates. (D and E) AsPC1 and BxPC3 cells were either unstimulated or stimulated with CpG (1 µM) for 24 h and levels of IL-6 (D) and IL-8 (E) in cell culture supernatants were quantified by cytometric bead array. (F) AsPC1 and BxPC3 cells were stimulated with CpG (1 µM) for 24 h and cellular proliferation was assessed using the XTT II assay (% proliferation was normalized to untreated control). (G) AsPC1 and BxPC3 cells were selectively stimulated with CpG (1 µM) for 24 h and Western blotting was performed on whole-cell lysates for select proteins involved in the regulation of pancreatic oncogenesis. Results were quantified based on triplicates. All experiments were reproduced two or three separate times. (H) Gene expression analysis using the preconfigured Human oncogene and tumor suppressor qPCR array was performed on AsPC1 and BxPC3 cells after 24-h treatment with CpG (1 µM). Fold-change compared with control untreated cells is shown (p = ns for all comparisons). PCR experiments were repeated twice with similar results (*, P < 0.05; **, P < 0.01; ***, P < 0.001 using the Student's t test).
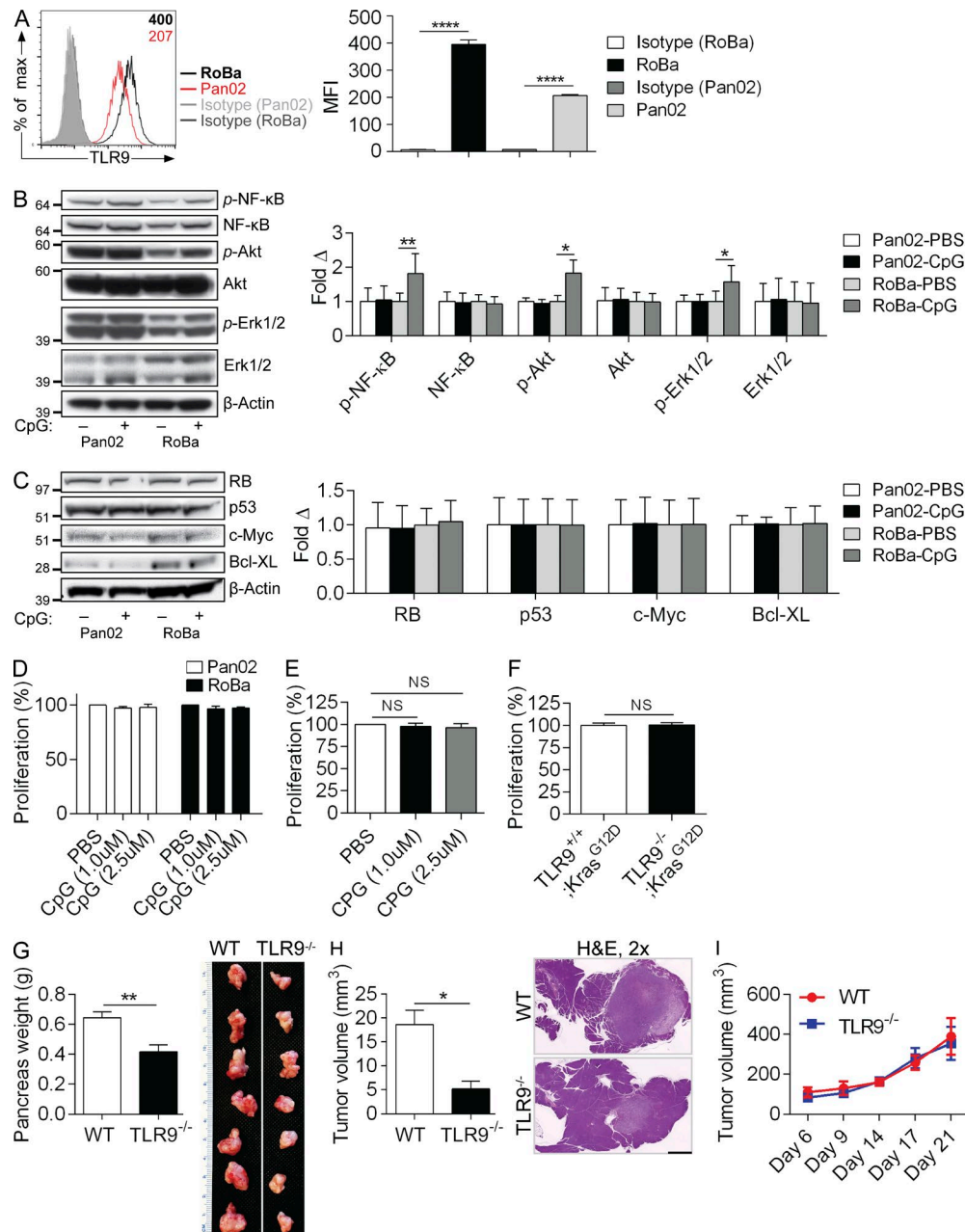
Figure 6. TLR9 ligation can be proinflammatory in murine pancreatic cancer cells but does not induce proliferative or oncogenic changes. (A) Pan02 cells and KPC-derived RoBa cells were tested for expression of TLR9 compared with isotype control. MFI is indicated in the upper right corner. Averages of tripli-cates based on MFI are shown. (B) Pan02 and RoBa cells were either unstimulated or stimulated with CpG (1 µM) for 10 min and tested for activation of inflam-matory signaling pathways by Western blotting. (C) Similarly, Pan02 and RoBa cells were selectively stimulated with CpG (1 µM) for 24 h and Western blotting was performed on whole-cell lysates for select proteins involved in the regulation of pancreatic oncogenesis. Results were quantified based on triplicates. (D) Pan02 and RoBa cells were stimulated with increasing doses of CpG and cellular proliferation was assessed using the XTT assay (p = ns for all comparisons). (E) Kras^{G12D}-PDEC were stimulated with increasing doses of CpG and proliferation measured as above (p = ns for all comparisons). (F) The comparative in vitro proliferation of TLR9$^{+/+}$;Kras^{G12D}-PDEC and TLR9$^{-/-}$;Kras^{G12D}-PDEC was tested using the XTT assay. In vitro experiments were performed in triplicate and repeated at least twice with similar results (*, P < 0.05; **, P < 0.01; ****, P < 0.0001). (G) WT and TLR9$^{-/-}$ mice were administered an orthotopic intrapancreatic injection of KPC-derived FC1242 cells. Tumors were harvested and weighed at 3 wk. Quantitative results and representative photographs of individual tumors are shown (n = 10/group; **, P < 0.01 using the Student's t test). (H) WT and TLR9$^{-/-}$ mice were administered an orthotopic intrapancreatic injection of TLR9$^{+/+}$;Kras^{G12D}-PDEC. Tumors were harvested at 3 wk. Quantitative results and representative H&E stained sections from each group are shown (n = 7/group; *, P < 0.05 using the Student's t test; 2; bar = 1 mm). (I) WT and TLR9$^{-/-}$ mice were administered a subcutaneous injection of FC1242 cells (n = 5/group). Tumor volume was calcu-lated at serial intervals by measuring the long (D) and short (d) diameter of the tumor, and applying the formula V = 1/2 × (D × d^2; p = ns at each time point).
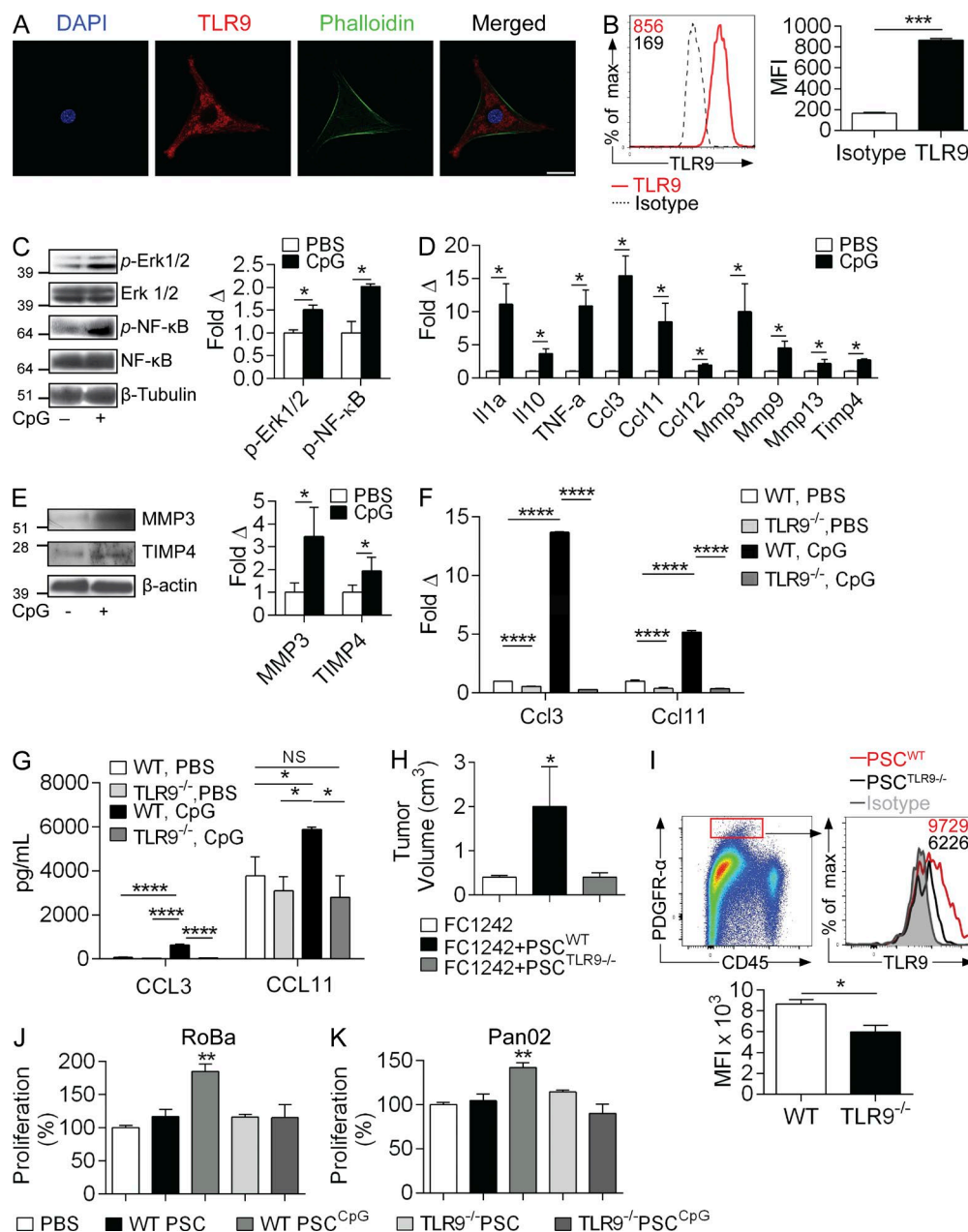
Figure 7. TLR9 ligation activates pancreatic stellate cells into protumorigenic entities. (A) Cultured PSCs were stained with DAPI, anti-TLR9 mAb, and phalloidin and imaged by confocal microscopy (63×; bar = 40 µm). (B) PSCs were also tested for expression of TLR9 by flow cytometry compared with isotype control. MFIs are indicated. Averages of triplicates based on MFI are shown. (C) PSCs were treated with CpG (1 µM) for 10 min and whole-cell lysates were tested for MAP kinase and NF-κB pathway activation by Western blotting. Density analysis was performed based on triplicates. (D) Gene expression analysis using the preconfigured mouse fibrosis qPCR array was performed on PSCs treated with CpG for 24 h. This experiment was repeated twice in triplicates. (E) Similarly, PSCs were treated with CpG for 24 h and whole-cell lysates were tested for MMP3 and TIMP4 by Western blotting. Results were quantified based on triplicates. (F) WT and TLR9$^{-/-}$ PSCs were treated for 24 h with CpG (1 µM), and expression of Ccl3 and Ccl11 mRNA were quantified by qPCR in triplicate. (G) Similarly, CCL3 and CCL11 protein levels were measured in cell culture supernatant of WT and TLR9$^{-/-}$ PSCs treated CpG versus untreated controls. Averages of triplicates are shown. (H and I) WT mice were orthotopically transplanted with FC1242 pancreatic cancer cells alone, FC1242 + PSCs derived from WT mice, or FC1242 + PSCs derived from TLR9$^{-/-}$ mice ($n = 4$/group). (H) Tumor volume was recorded at 3 wk. This experiment was performed twice with similar results. (I) PDGFR-α$^+$ CAFs from orthotopic FC1242 tumors that had been co-implanted with TLR9$^{+/+}$ and TLR9$^{-/-}$ PSCs were gated on flow cytometry and tested for expression of TLR9. Averages of quadruplicates are shown. RoBa (J) and Pan02 (K) cells were cultured for 24 h in 96-well plates with conditioned media derived from WT or TLR9$^{-/-}$ PSCs that had been either unstimulated or pretreated with CpG (1 µM). Cellular proliferation was assessed using the XTT assay based on triplicates. All experiments were repeated two to three times with similar results (*, P < 0.05; **, P < 0.01; ***, P < 0.001; ****, P < 0.0001 using the Student's *t* test or ANOVA).
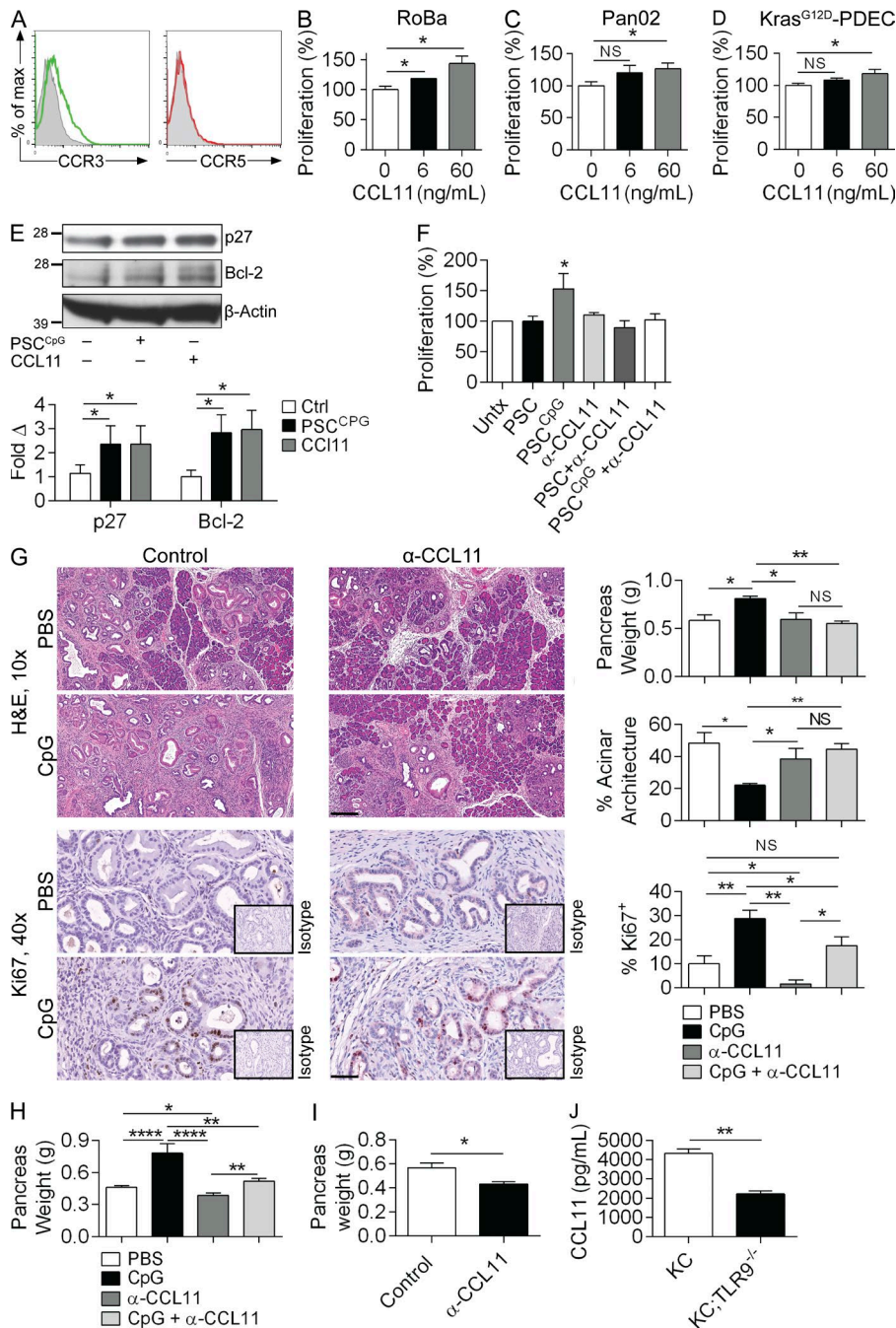
Figure 8. PSC-derived CCL11 promotes tumor progression. (A) Pan02 cells were tested by flow cytometry for expression of CCR3 and CCR5 compared with isotype control. RoBa cells (B), Pan02 cells (C), and Kras[G12D]-PDECs (D) were stimulated with recombinant murine CCL11 at the designated concentrations for 24 h in 96-well plates, and proliferation was assessed with the XTT assay. Averages of triplicates are shown. (E) Pan02 cells stimulated with recombinant CCL11 (60 ng/ml) or conditioned media derived from CpG-treated PSCs and tumor cell lysates were tested for p27 and Bcl-2 expression by Western blotting. (F) Pan02 cells were cultured alone or with conditioned media derived from untreated or CpG-treated WT PSCs in the presence or absence of α-CCL11–neutralizing antibody. Proliferation was measured at 24 h. Averages of triplicates are shown. All cellular proliferation experiments were repeated at least twice. (G) 10-wk-old KC mice were administered CpG or PBS for 4 wk, with or without concurrent administration of an α-CCL11 neutralizing antibody. Pancreata were weighed and assessed by H&E (10×; bar = 200 µm) and Ki67 IHC (40×; bar = 50 µm). The extent of morphological transformation and epithelial cell proliferation, respectively, were quantified (n = 4/group). (H) 8-wk-old KPC mice without palpable tumor were treated with CpG or PBS for 6 wk, with concurrent administration of an α-CCL11 neutralizing antibody or isotype control. Pancreata were weighed (n = 6/group). (I) WT mice were challenged with orthotopic KPC-derived FC1242 tumor and treated with α-CCL11 or control. Pancreata were harvested at 3 wk and weighed (n = 5/group). (J) Lysates from pancreata of 3-mo-old KC and KC;TLR9^{−/−} mice were tested for CCL11 levels by ELISA (n = 3/group; *, P < 0.05; **, P < 0.01; ****, P < 0.0001 using the Student's t test or ANOVA).

TLR9 signaling promotes regulatory T (T reg) cell and MDSC accumulation in the tumor microenvironment

We showed that TLR9 activation led to an augmentation of the intratumoral inflammatory infiltrate but failed to promote tumor rejection (Fig. 2). We postulated that this was attributable to the generation of an immunosuppressive microenvironment. The fraction of CD4^{+} and CD8^{+} T cells within the pancreas was unaltered by CpG treatment (Fig. 9 A). Nevertheless, we found that the influx of CD4^{+}CD25^{+}FoxP3^{+} T reg cells was elevated after CpG administration (Fig. 9 B). Pan-

creas-infiltrating T reg cells did not express TLR9 (Fig. 9 C). However, CCR5 ligation has been reported to be powerfully chemotactic for T reg cells in PDAC (Tan et al., 2009). Because CpG induces PSC production of CCL3, which ligates CCR5, we postulated that TLR9 signaling in PSCs may be necessary for the recruitment of T reg cells in PDAC. CCL3 was highly elevated in pancreata of CpG-treated KC mice (Fig. 9 D). To test our hypothesis that TLR9-activated PSCs induce T reg cell recruitment, we used our orthotopic tumor model using KPC-derived FC1242 cells. We found that com-

pared with orthotopic implantation of FC1242 cells alone, co-administration of FC1242 cells and WT PSCs resulted in a substantial increase in T reg cell recruitment and their expression of IL-10 (Fig. 9, E and F). In contrast, co-administration of FC1242 and TLR9$^{-/-}$ PSCs did not increase T reg cell recruitment to the TME nor did it affect their activation, suggesting that TLR9 signaling in PSCs promotes the recruitment of T reg cells to the pancreatic TME and augments their immunosuppressive cytokine response (Fig. 9, E and F). Consistent with this notion, conditioned media from CpG-activated PSCs differentially induced T reg polarization in vitro in bulk splenic CD4$^+$ T cells (Fig. 9 G).

We previously reported that MDSCs induce immune suppression in the pancreatic TME and promote metastases deposition by negating cytotoxic CD8$^+$ T cell responses (Connolly et al., 2010; Pylayeva-Gupta et al., 2012). However, trafficking of MDSCs to PDAC is incompletely understood. CCL11 has been shown to promote chemotaxis of eosinophils and mast cells by binding to CCR3, but its effects on MDSC recruitment remain unknown (Murdoch et al., 2008). We hypothesized that PSC-derived CCL11 recruits MDSCs to the TME of TLR9-stimulated KC mice. Accordingly, we found that the fraction of CD11b$^+$Gr1$^+$ MDSCs was substantially elevated after CpG administration (Fig. 9 H). In addition, CpG-treatment augmented the production of TNF by MDSCs (Fig. 9 I). However, MDSCs derived from PBS- or CpG-treated tumor had comparable capacity to inhibit T cell proliferation (Fig. 9 J), IL-6 (Fig. 9 K), TNF, and IFN-γ (not depicted) production. Intrapancreatic MDSCs uniformly expressed high CCR3 in contrast to minimal CCR5 (Fig. 9 L). Nevertheless, contrary to our hypothesis, in vivo CCL11 blockade did not mitigate the augmented MDSC recruitment in CpG-treated KC mice (unpublished data). Further, orthotopic administration of FC1242 + WT PSCs did not differentially increase MDSC recruitment compared with FC1242 cells alone or co-administration of FC1242 + TLR9$^{-/-}$ PSCs (Fig. 9 M). Collectively, these data suggest that neither CCL11 nor other secreted factors from TLR9-activated PSCs are responsible for MDSC recruitment to the PDAC TME. Because myeloid cells within the pancreatic TME express TLR9 (Fig. 1 B), we postulated that MDSCs may be recruited by direct TLR9 ligation. Consistent with this hypothesis, we found that KC;TLR9$^{-/-}$ mice contained reduced fractions of intrapancreatic MDSCs compared with KC mice (Fig. 9 N). Similarly, orthotopic FC1242 tumor administration to TLR9$^{-/-}$ mice resulted in a ~35% reduction in MDSC recruitment compared with orthotopic tumor administration to WT mice (unpublished data), indicating that TLR9 signaling in inflammatory cells supports MDSC accumulation in PDAC.

DISCUSSION

In this study, we investigated the role of TLR9 in the context of incipient pancreatic carcinogenesis. We show that TLR9 is widely expressed in pancreatic epithelial and surrounding stromal cells, even early during the course of transformation in mice. We further show that TLR9 ligation has complex protumorigenic effects in the pancreatic TME. Conversely, in various extrapancreatic tumor models, TLR activation has antitumor potential. For example, in glioma, renal cell cancer, and metastatic colon cancer TLR9 ligation is protective. Similar anticancer therapeutic results have been reported with selective TLR manipulation in melanoma (TLR7), CLL (TLR7, TLR8), breast cancer (TLR3, TLR5), and basal cell carcinoma (TLR7), among others (Butts et al., 2005; El Andaloussi et al., 2006; Salaun et al., 2006; Sfondrini et al., 2006; Chen et al., 2007; Kanzler et al., 2007; Spaner and Masellis, 2007). Antitumor effects of TLR activation are postulated to be performed by complementary mechanisms, including enhancing antigen presentation and subsequent CTL, potentiating innate immune responses, inducing the expression of tumoricidal cytokines, and directly causing apoptosis of cancer cells expressing specific TLR receptors (Kanzler et al., 2007). Although our data are seemingly paradoxical with these studies, additional recent studies have similarly shown that TLR ligation may promote oncogenesis (Tuomela et al., 2013; Chatterjee et al., 2014). We speculate that the tumor-modulatory effects of selective TLR activation may vary depending on the competing influences played by antitumor immunity versus tumor-promoting inflammation in each particular malignancy. Specifically, whereas TLR ligation can promote antitumor immune responses in otherwise tolerogenic microenvironments, in malignancies such as PDAC that are necessarily driven in their earliest stages by continued inflammation (Guerra et al., 2007), TLR signaling can induce tumor-promoting inflammatory signals. Quintessential examples of this concept in the extrapancreatic environment are ulcerative colitis–induced colon cancer and *Helicobacter pylori*–associated gastric cancer, diseases governed by a primary inflammatory component with an essential link between the proinflammatory milieu initiated by TLR activation and ensuing malignant transformation (Fukata et al., 2007; Fukata and Abreu, 2008).

Administration of TLR9 ligands to KC or KPC mice promoted acceleration of pancreatic transformation, accompanied by a pronounced desmoplastic reaction and an augmented inflammatory infiltrate. Further, TLR9 ligation resulted in activation of MAPK, NF-κB, and STAT3 pathways in vivo, as well as up-regulation of p53 and p27 and antiapoptotic and protumorigenic proteins such as Bcl-2, Bcl-X$_L$, c-Myc, and Cyclin D1 (Greten et al., 2002; Fukuda et al., 2011; Lesina et al., 2011; Huang et al., 2014). High p53 and p27 are associated with an aggressive tumor phenotype in PDAC, as we and others have shown, and likely represent an oncogene–induced senescence (OIS) signature (Caldwell et al., 2012; Ochi et al., 2012a). Conversely, genetic ablation of TLR9 had a tumor-protective effect, resulting in a decreased fraction of proliferating pancreatic ductal epithelial cells and improved overall survival in mice. Notably, TLR9 activation in the transformed epithelial cells was sufficient
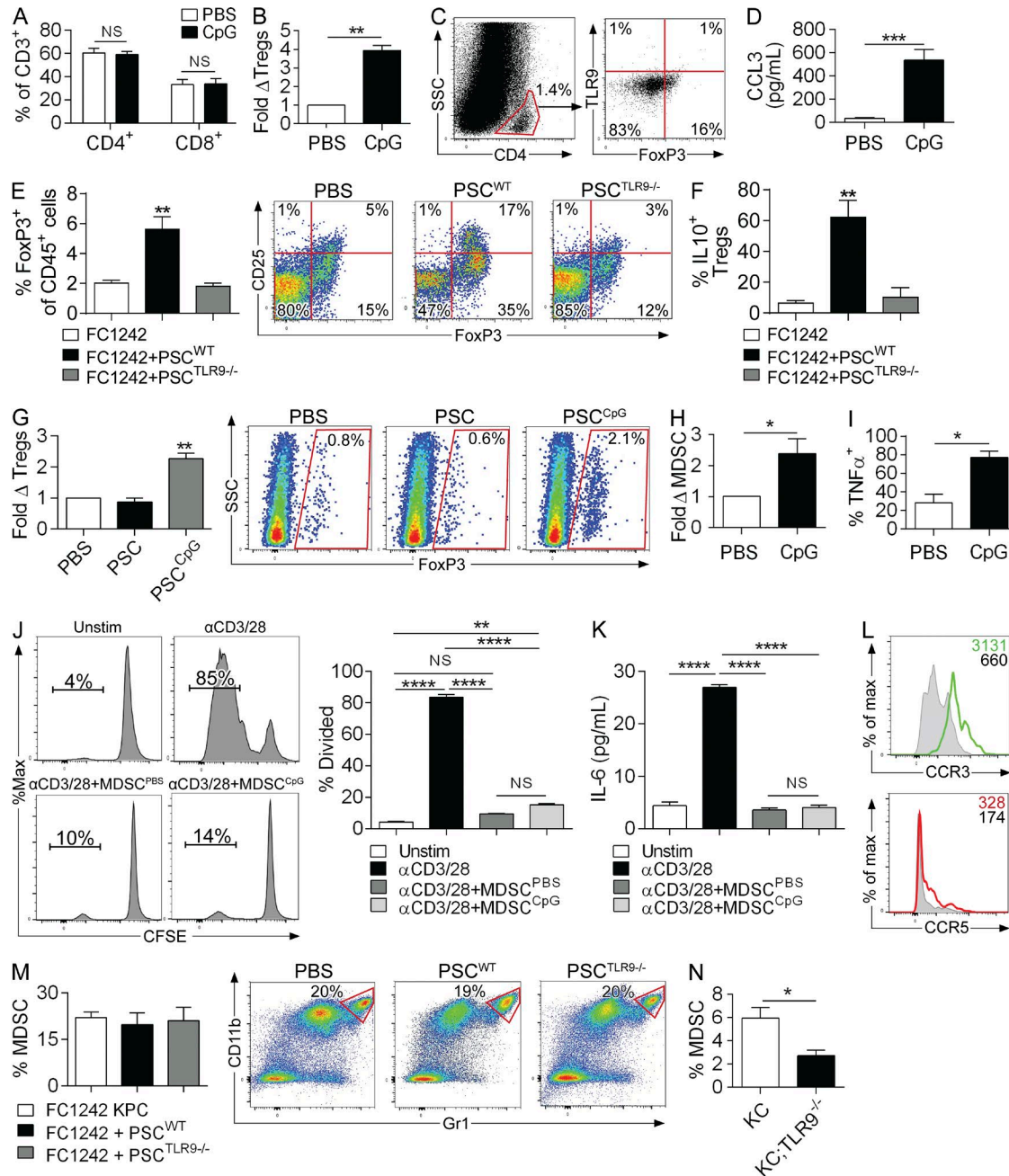
Figure 9. **TLR9 ligation recruits immune suppressive cellular subsets to the pancreatic tumor microenvironment.** (A and B) 10-wk-old KC mice were administered CpG or PBS thrice weekly for 4 wk and the frequency of intrapancreatic CD4$^+$ and CD8$^+$ T cells determined by flow cytometry ($n = 4$/group). (B) Similarly, the relative number of CD45$^+$CD3$^+$CD4$^+$FoxP3$^+$CD25$^+$ T reg cells was determined in PBS- and CpG-treated KC pancreata. (C) CD4$^+$ pancreatic T lymphocytes in KC mice were gated and tested for coexpression of FoxP3 and TLR9. (D) 10-wk-old KC mice were treated with PBS or CpG for 4 wk and CCL3 levels in pancreatic lysates were quantified using a cytometric bead array ($n = 3$/group). (E and F) WT mice were treated with an intrapancreatic injection of FC1242 cells alone, FC1242 + WT PSCs, or FC1242 + TLR9$^{-/-}$ PSCs ($n = 4$/group). (E) The percentage of CD3$^+$CD4$^+$FoxP3$^+$ pancreatic leukocytes among all CD45$^+$ leukocytes was calculated. Representative dot plots showing CD25 and FoxP3 coexpression on CD4$^+$ T cells are shown for each experimental group. (F) IL-10 expression was determined on CD4$^+$CD25$^+$FoxP3$^+$ T reg cells by intracellular cytokine analysis. (G) CD4$^+$ splenic T cells from WT mice were FACS-sorted and incubated alone or with conditioned media from PBS- or CpG-treated PSCs. On day 5, T cells were then tested for expression of FoxP3. Representative data and averages of quadruplicates are shown. (H and I) 10-wk-old KC mice were administered CpG or PBS thrice weekly for 4 wk ($n = 4$/group). (H) The percentage of CD45$^+$CD11b$^+$Gr1$^+$ MDSCs in each cohort was determined by flow cytometry. (I) Similarly, the production of TNF by intrapancreatic MDSC was quantified by intracellular cytokine staining in CpG- and PBS-treated KC mice. (J and K) Splenic T cells labeled with CFSE were cultured without stimulation, stimulated with αCD3 + αCD28 mAbs alone, αCD3 + αCD28 mAbs + MDSC harvested from PBS-treated KC mice, or αCD3 +

to induce the secretion of inflammatory mediators and selectively modulate proinflammatory signaling pathways, in contrast to TLR4 and TLR7, which have no direct effects on cancer cells (Ochi et al., 2012a,b). However, the observation that no alterations were observed in the phosphorylation status of NF-κB upon TLR9 stimulation in both human (BxPC3) and murine (Pan02) Kras-WT cell lines perhaps suggests that optimal TLR9 signal transduction in PDAC cells may require overactive Ras. In support of this, Xu et al. (2003) found that active Ras associates with TLR9 and overexpression of WT Ras enhances CpG-induced NF-κB signaling. Conversely, inhibition of Ras or overexpression of dominant-negative RasN17 inhibits CpG-induced cytokine responses and IRAK1–TRAF6 complex formation (Xu et al., 2003).

Because we found that several protumorigenic proteins were overexpressed after TLR9 ligation in vivo, and that TLR9-deficient KC mice had a decreased fraction of proliferating epithelial cells, we assessed the capacity of TLR9 to promote tumor cell proliferation in a cell-autonomous manner. TLR9 activation on epithelial cells did not have any direct effect on cellular proliferation in vitro, irrespective of Kras mutational status. We also did not observe any perturbation in oncogene or tumor-suppressor gene expression after TLR9 stimulation in murine or human PDAC cells. Therefore, the effects of TLR9 ligation on the transformed epithelial cells are not cell-autonomous and involve additional factors. Lending further support to this, we did not observe any deficits in cellular proliferation of TLR9$^{-/-}$;Kras^{G12D}-PDEC in vitro or in vivo. Further, the findings that TLR9$^{-/-}$ mice were not protected when pancreatic tumor was implanted subcutaneously suggested that effects were contingent on elements specific to the intrapancreatic microenvironment.

The robust stromal reaction observed after in vivo TLR9 ligation prompted us to investigate the role of the cancer-associated fibroblasts (CAFs) as mediators of the protumorigenic effects of TLR9. Using a previously reported flow cytometry marker (PDGFR-α; Erez et al., 2010), we found that CAFs express TLR9 in KC mice. Pancreatic CAFs are believed to originate from PSCs, which have been shown by others to express TLRs 2–5 (Masamune et al., 2008; Vonlaufen et al., 2010). However, PSC expression of TLR9 has not been reported. We found that cultured PSCs express high levels of TLR9 and respond vigorously to CpG by activating the MAPK and NF-κB pathways.

To investigate the biological significance of TLR9 signaling in PSCs during pancreatic oncogenesis, we used a previously described system of orthotopic co-injection of pancreatic cancer cells and PSCs (Vonlaufen et al., 2008). Although co-injection of KPC-derived tumor cells and PSCs led to a doubling in tumor size, TLR9-deficient PSCs were unable to support tumor growth. We validated this finding by culturing pancreatic cancer cells in the presence of conditioned media derived from CpG-stimulated PSCs, which augmented the proliferation of the cancer cells in a TLR9-dependent manner.

To determine the factors secreted by TLR9-activated PSCs responsible for the proproliferative effects of TLR9 on transformed pancreatic epithelial cells, we screened for an array of inflammation- and fibrosis-related genes and found that TLR9 ligation induces up-regulation of several cytokines, chemokines, and matrix metalloproteinases. IL-1α, TNF, and CCL2 have well-established protumorigenic roles in PDAC (Gukovsky et al., 2013; Zheng et al., 2013). Similarly, MMP3 and MMP9 promote PDAC invasion and hence may be in part responsible for the increased number of invasive foci observed after TLR9 stimulation in vivo (Bera et al., 2013; Mehner et al., 2014). Conversely, CCL3 and CCL11 have not been studied in the context of pancreatic carcinogenesis. We found that CpG stimulation of PSCs up-regulates the expression of the Ccl3 and Ccl11 genes and leads to increased secretion of soluble CCL3 and CCL11 in a TLR9-specific manner. Further, we show that CCL11 can promote the proliferation of PDAC cells in a dose-dependent manner, and CCL11 mediates the tumor-proliferative effect of TLR9-activated PSCs. Interestingly, CCL11 blockade slowed spontaneous tumor progression in the endogenous and orthotopic KPC models but not in the KC model. However, even in KC model CCL11 blockade diminished epithelial cell proliferation. Further, our correlative in vitro experiments using either recombinant CCL11 or CCL11 blockade show that CCL11 influences PDAC proliferation. Previous studies have shown that CCL11 can promote tumor progression in other cancer subtypes. In prostate cancer, CCL11 acts via CCR3 to accelerate tumor invasion and migration, which are dependent on ERK1/2 activation and MMP3 expression (Zhu et al., 2014). Accordingly, serum CCL11 levels are elevated in prostate cancer (Agarwal et al., 2013). CCL11 also induces phosphorylation of ERK1/2, MEK1, and STAT3 in ovarian carcinoma and stimulates

αCD28 mAbs + MDSC harvested from CpG-treated KC mice (5:1 T cell/MDSC ratio). (J) T cell proliferation was determined by dissolution of CFSE. (K) IL-6 was measured in cell culture supernatant by cytometric bead array. Representative data and averages of triplicates are shown. This experiment was performed twice. (L) CD45$^+$CD11b$^+$Gr1$^+$ cells from 3-mo-old KC mice were tested for expression of CCR3 and CCR5 by flow cytometry. Shaded histograms correspond to isotype controls. (M) WT mice were administered an intrapancreatic injection of FC1242 cells alone, FC1242 + WT PSCs, or FC1242 + TLR9$^{-/-}$ PSCs (n = 4/group). 3 wk later, the percentage of CD11b$^+$Gr1$^+$ MDSC among intratumoral CD45$^+$ cells was assessed by flow cytometry. Representative dot plots are shown for each experimental group (p = ns for all comparisons). (N) The percentage of CD11b$^+$Gr1$^+$ intrapancreatic MDSC among CD45$^+$ cells were quantified by flow cytometry in 3-mo-old KC and KC;TLR9$^{-/-}$ mice (n = 4/group). All data were reproduced in three separate experiments (*, P < 0.05; **, P < 0.01; ***, P < 0.001; ****, P < 0.0001 using the Student's t test or ANOVA).

tumor proliferation, migration, and invasion (Levina et al., 2009). Notably, sera from PDAC patients—used as controls in the ovarian cancer study—exhibit significantly elevated levels of CCL11 compared with sera of healthy individuals (Levina et al., 2009).

We previously reported that the KC model generates pancreas-specific T cell responses as intratumoral T cells become activated when restimulated with pancreas-derived antigen (Ochi et al., 2012b). However, the antitumorigenic T cells are maintained in an anergic state by components of the tumor microenvironment, thus permitting tumor progression. We observed that CpG-treated KC mice had elevated intrapancreatic levels of MDSCs as well as T reg cells, whereas TLR9$^{-/-}$;KC mice had reduced infiltration with immune suppressive cells. We previously showed that MDSCs critically disable cytotoxic T cells in PDAC and thereby promote tumor progression and liver metastases (Connolly et al., 2010; Pylayeva-Gupta et al., 2012). However, the respective mechanisms of TLR9-mediated recruitment and activation of MDSC and T reg cells was very different. Intrapancreatic MDSCs expressed high levels of TLR9, and genetic ablation of TLR9 in KC mice led to decreased infiltration of MDSCs into the pancreas. Nevertheless, despite high MDSC expression of CCR3, TLR9-activated PSCs did not promote their recruitment. TLRs have similarly been shown to modulate MDSC infiltration in the context of infectious and allergic disease as part of a homeostatic mechanism against overwhelming inflammation (Ray et al., 2013). In contrast to MDSC, T reg cells did not express TLR9. Instead, TLR9 activation led to recruitment and activation of T reg cells indirectly, through PSC-dependent pathways. Specifically, we show that TLR9-competent PSCs induce an increase of intratumoral T reg cells and augment their IL-10 production, whereas TLR9-deficient PSCs have no effect. PSC-derived CCL3 may be responsible for the increased influx of T reg cells after TLR9 activation. This is justified by a previous report suggesting that CCR5 signaling promotes T reg cell recruitment in tumors (Schlecker et al., 2012). Further, blockade of CCR5 signaling disrupts T reg cell homing and inhibits tumor growth in orthotopic models of PDAC (Tan et al., 2009). Besides TLR9-activated PSCs, another potential source of CCR5 ligands in the pancreatic TME may be MDSCs, as has been reported in other malignancies (Schlecker et al., 2012). Gabitass et al. (2011) even found that the number of T reg cells in the peripheral blood of PDAC patients correlates positively with the numbers of MDSCs.

In summary, this study provides evidence for the prooncogenic role of TLR9 in PDACs through complementary modalities that both promote tumor cell proliferation and perpetuate intratumoral immune-suppression. Our findings place the PSCs at a central position in this network. From a translational standpoint, we describe a novel role for PSC-derived CCL11 as a soluble factor driving PDAC tumor growth, and therefore it constitutes an attractive new target for experimental therapeutics.

MATERIALS AND METHODS

Animals. C57BL/6 (H-2Kb) mice were purchased from The Jackson Laboratory. TLR9$^{-/-}$ mice were a gift from S. Akira (Osaka University, Osaka, Japan) and have been described previously (Hemmi et al., 2000). KC mice were generated by crossing LSL-Kras$^{G12D/+}$ mice with p48$^{+/Cre}$ mice (Hingorani et al., 2003). KC;TLR9$^{-/-}$ mice were generated by crossing LSL-Kras$^{G12D/+}$;TLR9$^{-/-}$ mice with p48$^{+/Cre}$;TLR9$^{-/-}$ mice. KPC mice (Hingorani et al., 2005) were a gift from M. Phillips (New York University, New York, NY). Animals were housed in a clean vivarium and fed standard mouse chow.

Pancreatic stellate cell isolation and culture. To generate PSCs, pancreata were dissected and pooled together in a culture dish containing GBSS (Sigma-Aldrich), washed, and finely minced. After centrifugation to remove excess fat, tissue was resuspended in a solution containing Collagenase P, Pronase, and DNase I (all from Roche) and incubated at 37°C for 50 min, with shaking every 5 min. Digested tissue was then strained and quenched with cold GBSS with 0.3% BSA and further centrifuged at 1,000 rpm for 10 min. The pellet was resuspended in 9.5 ml GBSS with 0.3% BSA and 8 ml of 28.7% Nycodenz gradient solution (Sigma-Aldrich), layered underneath GBSS, and centrifuged at 1,400 g for 20 min. PSCs were collected from the fuzzy band at the interface, washed with GBSS, resuspended in growth medium (DMEM/F12 supplemented with 10% FBS, penicillin, streptomycin, and L-Glutamine), and plated at a density of 40,000 cells/cm^2. Growth medium was replaced the day after initial seeding and, subsequently, every 3 d. Cells were split when 80% confluency was reached. The purity of PSC cultures were confirmed by GFAP and α–SMA immunofluorescent staining after the second passage, as we and others have shown (Vonlaufen et al., 2010; Ibrahim et al., 2012). Experiments were performed between passages three and five.

Pancreatic cancer cell lines and 3D cultures. The human PDAC cell lines AsPC1 and BxPC3 (gifts from D. Bar-Sagi, New York University, New York, NY) and murine Pan02 cell line (gift from D. Meruelo, New York University, New York, NY) were maintained in complete RPMI (RPMI-1640 with 10% heat-inactivated FBS, 2 mM L-glutamine, and 0.05 mM 2-ME). Kras^{G12D}-PDEC were harvested by microdissection of the pancreatic ducts of KC mice and propagated in 3D cultures, as previously described (Pylayeva-Gupta et al., 2012). Murine RoBa (mixed background) and FC1242 (C57BL/6 background) cells were generated from KPC mice as described previously, with modifications (Schreiber et al., 2004). In brief, pancreatic tumors were harvested from 6-mo-old KPC mice and minced in DMEM with 2 mg/ml Collagenase V. Suspensions were incubated at 37°C for 45 min with shaking, centrifuged at 900 rpm, and resuspended in DMEM with 10% FBS. Cells were split at 1:100 to dilute out stromal cell contamination, which does not tolerate aggressive splitting. In

select experiments, murine cells were stimulated with CpG ODN1826 (1–2.5 µM) or recombinant murine CCL11 (6-60 ng/ml; R&D Systems) and human cells were stimulated with CpG ODN2006 (2.5 µM; InvivoGen). Proliferation in response to various stimuli was assessed using the XTT II assay according to the manufacturer's protocol (Cell Proliferation kit II; Roche).

In vivo experiments. To study the effects of TLR9 ligation, KC or KPC mice were administered CpG ODN1826 (InvivoGen) by i.p. injection (31.75 µg) or oral gavage (127 µg) thrice weekly for various durations, depending on the experiment. In selected experiments, mice were treated with a CCL11 neutralizing mAb (10 µg, i.p., twice weekly; Clone 42285; R&D Systems) or isotype control. For experiments involving KPC mice, to ensure uniformity, animals with palpable tumors at 8 wk of age were excluded from entry into experiments. To track CpG in vivo, WT mice were induced to develop caerulein (50 µg/kg; Sigma-Aldrich) pancreatitis for 48 h before administration of FITC-labeled CpG ODN1826 (25 µg; InvivoGen) via oral gavage. Mice were sacrificed 6 h later and the presence of CpG in the pancreas was determined by flow cytometry. For additional experiments, mice were administered *Streptococcus mutans UA159* (*S. mutans*; 10^8 cells) i.p. or by oral gavage after labeling the bacteria with CellTrace CFSE (Life Technologies) according to the manufacturer's protocols. Recipient mice were sacrificed at 6 h. For orthotopic injections, tumor cells were suspended in PBS with Matrigel (BD) in a 1:1 ratio and $Kras^{G12D}$–PDEC (10^6 cells) or KPC–derived FC1242 cells (10^5) were injected into the body of the pancreas via laparotomy. In select experiments, an equal number of PSCs were administered along with the FC1242 cells. In select experiments, tumor cells were administered subcutaneously at the same doses. Mice were sacrificed 3 wk later and tumor volume was recorded. All animal procedures were approved by the NYU School of Medicine IACUC.

Protein extraction and immunoblotting. Protein extraction from adherent cells was performed by aspirating cell culture supernatant, immediately adding ice-cold RIPA buffer with complete protease inhibitor cocktail and *phosSTOP* phosphatase inhibitor cocktail (Roche), incubating for 30 min on ice with gentle vortexing every 5 min, centrifuging at 14,000 *g* for 15 min, and collecting the supernatant. For protein extraction from tissues, 15–30 mg of tissue were homogenized in 150–300 µl ice-cold RIPA buffer and subsequently processed in the same way as centrifugation and supernatant collection. Total protein was quantified using the DC Protein Assay (Bio-Rad Laboratories) according to the manufacturer's instructions. Western blotting was performed as previously described, with minor modifications (Ochi et al., 2012a). In brief, 10% Bis-Tris polyacrylamide gels (NuPage; Invitrogen) were equiloaded with 10–30 µg of protein, electrophoresed

at 200 V, and electrotransferred to PVDF membranes. After blocking with 5% BSA, membranes were probed with primary antibodies to β–actin (polyclonal), MMP3 (EP1186Y), TIMP4 (SB30c), p27 (EP233(2)Y, mouse; all from Abcam); c-Myc (9E10), Cyclin B1 (GNS1), Cyclin D1 (M–20), RB (C-15; all from Santa Cruz Biotechnology, Inc.); p27 (D69C12, human), Bcl-2 (50E3), NF-κB/p65 (L8F6), p-NF-κB/p65 (93H1), Akt (40D4), p-Akt (C31E5E), c-jun (KM-1), Erk1/2 (137F5), p-Erk1/2 (D13.14.4E), β-Tubulin (9F3), Bcl-X$_L$ (54H6), p53 (PAb 240), STAT3 (79D7), p-STAT3 (D3A7; all from Cell Signaling Technology); and Ezrin (3C12; BD). Blots were developed using ECL (Thermo Fisher Scientific).

RT–PCR. RNA extraction was performed using the RNeasy Mini kit (QIAGEN) as per the manufacturer's instructions. RNA was converted to cDNA using the RT^2 First Strand kit (QIAGEN). qPCR was performed using the RT^2 SYBR Green qPCR Mastermix (QIAGEN) on the Stratagene MX3005P (Stratagene). The following forward (F) and reverse (R) primers were used: F, 5′-AATCGTGCGTGAC ATCAAAG-3′ and R, 5′-ATGCCACAGGATTCCATA CC-3′ for mouse β-actin (Li et al., 2011); F, 5′-GTACCATG ACACTCTGCAACC-3′ and R, 5′-GTCAGGAAAATGA CACCTGGC-3′ for mouse Ccl3 (Volat et al., 2012); F, 5′- TGGGATGCCTTTGTGGAACT-3′ and R, 5′-ACA GCCAGGAGAAATCAAACAG-3′ for mouse Bcl2 (Mohrin et al., 2010); F, 5′-GGCTGGGACACTTTTGTG GAT-3′ and R, 5′-GCGCTCCTGGCCTTTCC-3′ for mouse Bcl2l1 (Bcl-xL; Mohrin et al., 2010); F, 5′-GGA CCTCGAGTGTGAAGCAT-3′ and R, CTGGAGCT CACAGGGTAGGA-3′ for human Tlr9; F, 5′-CTGTGGCA TCCACGAAACTA-3′ and R, 5′-AGTACTTGCGCTC AGGAGGA-3′ for human β-actin (Ho-Pun-Cheung et al., 2009). For mouse Ccl11, predesigned primers were purchased from QIAGEN. Expression levels were normalized to β-actin and expressed as fold change compared with control. In selected experiments, the Human Oncogenes and Tumor Suppressor Genes and Mouse Fibrosis standardized preconfigured qPCR arrays were used (QIAGEN).

T cell assays and cytokine and chemokine analysis. In vitro T cell activation was accomplished by labeling spleen-derived T cell with CFSE and activating cells in 96-well plates for 72 h using plate-bound αCD3 (10 µg/ml) + αCD28 (5 µg/ml; both from BioLegend) mAbs. In select wells, FACS-sorted pancreatic CD11b$^+$Gr1$^+$ cells were added in a 5:1 T cell/ MDSC ratio as described (Connolly et al., 2010; Pylayeva-Gupta et al., 2012). T cell proliferation was determined by dissolution of CFSE. For quantification of CCL11, the mouse CCL11 DuoSet ELISA kit (R&D Systems) was used per the manufacturer's protocols. For all other cytokines and chemokines, the Cytometric Bead Array Mouse Inflammation kit or Mouse Flex Set kit (both from BD) were used according to manufacturer's protocols.

Flow cytometry. Single-cell suspensions for flow cytometry were prepared as described previously with slight modifications (Ochi et al., 2012a). In brief, pancreata were harvested immediately after mouse sacrifice and placed in cold RPMI1640 with 1 mg/ml Collagenase IV (Worthington Biochemical) and 2 U/ml DNase I (Promega). After mincing with scissors to sub-millimeter pieces, tissues were incubated at 37°C for 30 min, with gentle shaking every 5 min. Specimens were passed through a 100 µm mesh, and centrifuged at 350g for 5 min. The cell pellet was resuspended in PBS with 1% FBS. After blocking FcγRIII/II with an anti-CD16/CD32 mAb (eBioscience), cell labeling was performed by incubating 10^6 cells with 1 µg of fluorescently conjugated antibodies directed against CD34 (RAM34; BD); CD45 (30-F11), CD133 (315-2C11), MHC II (M5/114.15.2), CD11c (N418), Ly-6C (HK1.4), Ly-6G (1A8), CD11b (M1/70), F4/80 (BM8), Gr1 (RB6-8C5), CD3 (17A2), CD4 (RM4-5), CD8 (53–6.7), FoxP3 (150D), CD25 (PC61), IL-10 (JES5-16E3), TNF (MP6-XT22), PDGFR-α/CD140 (APA5), CCR3 (J073E5), CCR5 (HM-CCR5, all BioLegend), and TLR9 (26C593.2; Novus Biologicals). Intracellular cytokine staining and intracellular FoxP3 staining were performed using the FixPerm kit (BD) and the FoxP3/Transcription Factor Staining kit (eBioscience), respectively. The FixPerm kit was also used for TLR9 staining. Flow cytometry was performed on either the LSR-II or the FACSCalibur (BD). Data were analyzed using FlowJo software (Tree Star).

Histology, immunohistochemistry, and microscopy. For histological analysis, pancreatic specimens were fixed with 10% buffered formalin, dehydrated in ethanol, embedded with paraffin, and stained with H&E or Trichrome. The fraction of preserved acinar area was calculated as previously described (Ochi et al., 2012a). The fraction and number of ducts containing all grades of PanIN lesions was measured by examining 10 HPFs per slide. PanINs were graded according to established criteria (Hruban et al., 2001). In brief, in PanIN I ducts, the normal cuboidal pancreatic epithelial cells transition to columnar architecture (PanIN Ia) and gain polyploid morphology (PanIN Ib). PanIN II lesions are associated with loss of polarity. PanIN III lesions show cribriforming, budding off of cells, and luminal necrosis with marked cytological abnormalities, without invasion beyond the basement membrane. Immunohistochemistry (IHC) was performed using antibodies directed against CD45 (polyclonal; Abcam), and Ki67 (SP6; Abcam). All quantifications were performed by assessing 10 high-power fields (HPF; 40×) per specimen. For analysis of human tissues, de-identified paraffin-embedded human pancreatic cancer specimens were probed with antibodies directed against TLR9 (26C593.2; Novus Biologicals) or HMGB1 (polyclonal; Abcam). All human tissues were collected using an internal review board–approved protocol. For confocal microscopy, cells were cultured on glass coverslips, fixed with 10% paraformaldehyde, and subsequently stained with anti-TLR9 (26C593.2; Novus Biologicals), DAPI (Vector Labs), and Phalloidin (Life Technologies). Immunofluorescent staining of mouse tissues was performed similarly on 5-µm frozen sections. Images were acquired using the LSM700 confocal microscope along with ZEN 2010 software (Carl Zeiss).

Statistical analysis. Statistical significance was determined by the two-tailed Student's t test or ANOVA using Prism software (GraphPad). Survival was analyzed according to the Kaplan-Meier method using the Gehan-Breslow-Wilcoxon Test. Data are presented as mean ± SEM. $P < 0.05$ was considered significant.

REFERENCES

Agarwal, M., C. He, J. Siddiqui, J.T. Wei, and J.A. Macoska. 2013. CCL11 (eotaxin-1): a new diagnostic serum marker for prostate cancer. *Prostate*. 73:573–581. http://dx.doi.org/10.1002/pros.22597

American Cancer Society. 2013. Cancer Facts & Figures 2013. In American Cancer Society, Atlanta.

Bartsch, D.K., T.M. Gress, and P. Langer. 2012. Familial pancreatic cancer--current knowledge. *Nat. Rev. Gastroenterol. Hepatol.* 9:445–453. http://dx.doi.org/10.1038/nrgastro.2012.111

Bera, A., S. Zhao, L. Cao, P.J. Chiao, and J.W. Freeman. 2013. Oncogenic K-Ras and loss of Smad4 mediate invasion by activating an EGFR/NF-κB Axis that induces expression of MMP9 and uPA in human pancreas progenitor cells. *PLoS One.* 8:e82282. http://dx.doi.org/10.1371/journal.pone.0082282

Butts, C., N. Murray, A. Maksymiuk, G. Goss, E. Marshall, D. Soulières, Y. Cormier, P. Ellis, A. Price, R. Sawhney, et al. 2005. Randomized phase IIB trial of BLP25 liposome vaccine in stage IIIB and IV non-small–cell lung cancer. *J. Clin. Oncol.* 23:6674–6681. http://dx.doi.org/10.1200/JCO.2005.13.011

Caldwell, M.E., G.M. DeNicola, C.P. Martins, M.A. Jacobetz, A. Maitra, R.H. Hruban, and D.A. Tuveson. 2012. Cellular features of senescence during the evolution of human and murine ductal pancreatic cancer. *Oncogene.* 31:1599–1608. http://dx.doi.org/10.1038/onc.2011.350

Chatterjee, S., L. Crozet, D. Damotte, K. Iribarren, C. Schramm, M. Alifano, A. Lupo, J. Cherfils-Vicini, J. Goc, S. Katsahian, et al. 2014. TLR7 promotes tumor progression, chemotherapy resistance, and poor clinical outcomes in non-small cell lung cancer. *Cancer Res.* 74:5008–5018. http://dx.doi.org/10.1158/0008-5472.CAN-13-2698

Chen, K., J. Huang, W. Gong, P. Iribarren, N.M. Dunlop, and J.M. Wang. 2007. Toll-like receptors in inflammation, infection and cancer. *Int. Immunopharmacol.* 7:1271–1285. http://dx.doi.org/10.1016/j.intimp.2007.05.016

Connolly, M.K., J. Mallen-St Clair, A.S. Bedrosian, A. Malhotra, V. Vera, J. Ibrahim, J. Henning, H.L. Pachter, D. Bar-Sagi, A.B. Frey, and G. Miller. 2010. Distinct populations of metastases-enabling myeloid cells expand in the liver of mice harboring invasive and preinvasive intra-abdominal tumor. *J. Leukoc. Biol.* 87:713–725. http://dx.doi.org/10.1189/jlb.0909607

Deer, E.L., J. González-Hernández, J.D. Coursen, J.E. Shea, J. Ngatia, C.L. Scaife, M.A. Firpo, and S.J. Mulvihill. 2010. Phenotype and genotype of pancreatic cancer cell lines. *Pancreas.* 39:425–435. http://dx.doi.org/10.1097/MPA.0b013e3181c15963

El Andaloussi, A., A.M. Sonabend, Y. Han, and M.S. Lesniak. 2006. Stimulation of TLR9 with CpG ODN enhances apoptosis of glioma and prolongs the survival of mice with experimental brain tumors. *Glia.* 54:526–535. http://dx.doi.org/10.1002/glia.20401

Erez, N., M. Truitt, P. Olson, S.T. Arron, and D. Hanahan. 2010. Cancer-associated fibroblasts are activated in incipient neoplasia to orchestrate tumor-promoting inflammation in an NF-kappaB–dependent manner. *Cancer Cell.* 17:135–147. http://dx.doi.org/10.1016/j.ccr.2009.12.041

Fukata, M., and M.T. Abreu. 2008. Role of Toll-like receptors in gastrointestinal malignancies. *Oncogene.* 27:234–243. http://dx.doi.org/10.1038/sj.onc.1210908

Fukata, M., A. Chen, A.S. Vamadevan, J. Cohen, K. Breglio, S. Krishnareddy, D. Hsu, R. Xu, N. Harpaz, A.J. Dannenberg, et al. 2007. Toll-like receptor-4 promotes the development of colitis-associated colorectal tumors. *Gastroenterology.* 133:1869–1881. http://dx.doi.org/10.1053/j.gastro.2007.09.008

Fukuda, A., S.C. Wang, J.P. Morris IV, A.E. Folias, A. Liou, G.E. Kim, S. Akira, K.M. Boucher, M.A. Firpo, S.J. Mulvihill, and M. Hebrok. 2011. Stat3 and MMP7 contribute to pancreatic ductal adenocarcinoma initiation and progression. *Cancer Cell.* 19:441–455. http://dx.doi.org/10.1016/j.ccr.2011.03.002

Gabitass, R.F., N.E. Annels, D.D. Stocken, H.A. Pandha, and G.W. Middleton. 2011. Elevated myeloid-derived suppressor cells in pancreatic, esophageal and gastric cancer are an independent prognostic factor and are associated with significant elevation of the Th2 cytokine interleukin-13. *Cancer Immunol. Immunother.* 60:1419–1430. http://dx.doi.org/10.1007/s00262-011-1028-0

Greten, F.R., C.K. Weber, T.F. Greten, G. Schneider, M. Wagner, G. Adler, and R.M. Schmid. 2002. Stat3 and NF-kappaB activation prevents apoptosis in pancreatic carcinogenesis. *Gastroenterology.* 123:2052–2063. http://dx.doi.org/10.1053/gast.2002.37075

Guerra, C., A.J. Schuhmacher, M. Cañamero, P.J. Grippo, L. Verdaguer, L. Pérez-Gallego, P. Dubus, E.P. Sandgren, and M. Barbacid. 2007. Chronic pancreatitis is essential for induction of pancreatic ductal adenocarcinoma by K-Ras oncogenes in adult mice. *Cancer Cell.* 11:291–302. http://dx.doi.org/10.1016/j.ccr.2007.01.012

Gukovsky, I., N. Li, J. Todoric, A. Gukovskaya, and M. Karin. 2013. Inflammation, autophagy, and obesity: common features in the pathogenesis of pancreatitis and pancreatic cancer. *Gastroenterology.* 144:1199–209.e4. http://dx.doi.org/10.1053/j.gastro.2013.02.007

Hemmi, H., O. Takeuchi, T. Kawai, T. Kaisho, S. Sato, H. Sanjo, M. Matsumoto, K. Hoshino, H. Wagner, K. Takeda, and S. Akira. 2000. A Toll-like receptor recognizes bacterial DNA. *Nature.* 408:740–745. http://dx.doi.org/10.1038/35047123

Hingorani, S.R., E.F. Petricoin, A. Maitra, V. Rajapakse, C. King, M.A. Jacobetz, S. Ross, T.P. Conrads, T.D. Veenstra, B.A. Hitt, et al. 2003. Preinvasive and invasive ductal pancreatic cancer and its early detection in the mouse. *Cancer Cell.* 4:437–450. http://dx.doi.org/10.1016/S1535-6108(03)00309-X

Hingorani, S.R., L. Wang, A.S. Multani, C. Combs, T.B. Deramaudt, R.H. Hruban, A.K. Rustgi, S. Chang, and D.A. Tuveson. 2005. Trp53R172H and KrasG12D cooperate to promote chromosomal instability and widely metastatic pancreatic ductal adenocarcinoma in mice. *Cancer Cell.* 7:469–483. http://dx.doi.org/10.1016/j.ccr.2005.04.023

Hirata, Y., H. Kurobe, M. Higashida, D. Fukuda, M. Shimabukuro, K. Tanaka, Y. Higashikuni, T. Kitagawa, and M. Sata. 2013. HMGB1 plays a critical role in vascular inflammation and lesion formation via toll-like receptor 9. *Atherosclerosis.* 231:227–233. http://dx.doi.org/10.1016/j.atherosclerosis.2013.09.010

Ho-Pun-Cheung, A., C. Bascoul-Mollevi, E. Assenat, F. Boissière-Michot, F. Bibeau, D. Cellier, M.Ychou, and E. Lopez-Crapez. 2009. Reverse transcription-quantitative polymerase chain reaction: description of a RIN-based algorithm for accurate data normalization. *BMC Mol. Biol.* 10:31. http://dx.doi.org/10.1186/1471-2199-10-31

Hruban, R.H., N.V. Adsay, J. Albores-Saavedra, C. Compton, E.S. Garrett, S.N. Goodman, S.E. Kern, D.S. Klimstra, G. Klöppel, D.S. Longnecker, et al. 2001. Pancreatic intraepithelial neoplasia: a new nomenclature and classification system for pancreatic duct lesions. *Am. J. Surg. Pathol.* 25:579–586. http://dx.doi.org/10.1097/00000478-200105000-00003

Huang, H., J. Daniluk, Y. Liu, J. Chu, Z. Li, B. Ji, and C.D. Logsdon. 2014. Oncogenic K-Ras requires activation for enhanced activity. *Oncogene.* 33:532–535. http://dx.doi.org/10.1038/onc.2012.619

Ibrahim, J., A.H. Nguyen, A. Rehman, A. Ochi, M. Jamal, C.S. Graffeo, J.R. Henning, C.P. Zambirinis, N.C. Fallon, R. Barilla, et al. 2012. Dendritic cell populations with different concentrations of lipid regulate tolerance and immunity in mouse and human liver. *Gastroenterology.* 143:1061–1072. http://dx.doi.org/10.1053/j.gastro.2012.06.003

Kanzler, H., F.J. Barrat, E.M. Hessel, and R.L. Coffman. 2007. Therapeutic targeting of innate immunity with Toll-like receptor agonists and antagonists. *Nat. Med.* 13:552–559. http://dx.doi.org/10.1038/nm1589

Lesina, M., M.U. Kurkowski, K. Ludes, S. Rose-John, M. Treiber, G. Klöppel, A. Yoshimura, W. Reindl, B. Sipos, S. Akira, et al. 2011. Stat3/Socs3 activation by IL-6 transsignaling promotes progression of pancreatic intraepithelial neoplasia and development of pancreatic cancer. *Cancer Cell.* 19:456–469. http://dx.doi.org/10.1016/j.ccr.2011.03.009

Levina, V., B.M. Nolen, A.M. Marrangoni, P. Cheng, J.R. Marks, M.J. Szczepanski, M.E. Szajnik, E. Gorelik, and A.E. Lokshin. 2009. Role of eotaxin-1 signaling in ovarian cancer. *Clin. Cancer Res.* 15:2647–2656. http://dx.doi.org/10.1158/1078-0432.CCR-08-2024

Li, S., A.L. Symonds, B. Zhu, M. Liu, M.V. Raymond, T. Miao, and P. Wang. 2011. Early growth response gene-2 (Egr-2) regulates the development of B and T cells. *PLoS One.* 6:e18498. http://dx.doi.org/10.1371/journal.pone.0018498

Masamune, A., K. Kikuta, T. Watanabe, K. Satoh, A. Satoh, and T. Shimosegawa. 2008. Pancreatic stellate cells express Toll-like receptors. *J. Gastroenterol.* 43:352–362. http://dx.doi.org/10.1007/s00535-008-2162-0

Mehner, C., E. Miller, D. Khauv, A. Nassar, A.L. Oberg, W.R. Bamlet, L. Zhang, J. Waldmann, E.S. Radisky, H.C. Crawford, and D.C. Radisky. 2014. Tumor cell-derived MMP3 orchestrates Rac1b and tissue alterations that promote pancreatic adenocarcinoma. *Mol. Cancer Res.* 12:1430–1439. http://dx.doi.org/10.1158/1541-7786.MCR-13-0557-T

Mohrin, M., E. Bourke, D. Alexander, M.R. Warr, K. Barry-Holson, M.M. Le Beau, C.G. Morrison, and E. Passegué. 2010. Hematopoietic stem cell quiescence promotes error-prone DNA repair and mutagenesis. *Cell Stem Cell.* 7:174–185. http://dx.doi.org/10.1016/j.stem.2010.06.014

Murdoch, C., M. Muthana, S.B. Coffelt, and C.E. Lewis. 2008. The role of myeloid cells in the promotion of tumour angiogenesis. *Nat. Rev. Cancer.* 8:618–631. http://dx.doi.org/10.1038/nrc2444

Ochi, A., C.S. Graffeo, C.P. Zambirinis, A. Rehman, M. Hackman, N. Fallon, R.M. Barilla, J.R. Henning, M. Jamal, R. Rao, et al. 2012a. Toll-like receptor 7 regulates pancreatic carcinogenesis in mice and humans. *J. Clin. Invest.* 122:4118–4129. http://dx.doi.org/10.1172/JCI63606

Ochi, A., A.H. Nguyen, A.S. Bedrosian, H.M. Mushlin, S. Zarbakhsh, R. Barilla, C.P. Zambirinis, N.C. Fallon, A. Rehman, Y. Pylayeva-Gupta, et al. 2012b. MyD88 inhibition amplifies dendritic cell capacity to promote pancreatic carcinogenesis via Th2 cells. *J. Exp. Med.* 209:1671–1687. http://dx.doi.org/10.1084/jem.20111706

Pylayeva-Gupta, Y., K.E. Lee, C.H. Hajdu, G. Miller, and D. Bar-Sagi. 2012. Oncogenic Kras-induced GM-CSF production promotes the development of pancreatic neoplasia. *Cancer Cell.* 21:836–847. http://dx.doi.org/10.1016/j.ccr.2012.04.024

Ray, A., K. Chakraborty, and P. Ray. 2013. Immunosuppressive MDSCs induced by TLR signaling during infection and role in resolution of inflammation. *Front. Cell. Infect. Microbiol.* 3:52. http://dx.doi.org/10.3389/fcimb.2013.00052

Salaun, B., I. Coste, M.C. Rissoan, S.J. Lebecque, and T. Renno. 2006. TLR3 can directly trigger apoptosis in human cancer cells. *J. Immunol.* 176:4894–4901. http://dx.doi.org/10.4049/jimmunol.176.8.4894

Schlecker, E., A. Stojanovic, C. Eisen, C. Quack, C.S. Falk, V. Umansky, and A. Cerwenka. 2012. Tumor-infiltrating monocytic myeloid-derived suppressor cells mediate CCR5-dependent recruitment of regulatory T cells favoring tumor growth. *J. Immunol.* 189:5602–5611. http://dx.doi.org/10.4049/jimmunol.1201018

Schreiber, F.S., T.B. Deramaudt, T.B. Brunner, M.I. Boretti, K.J. Gooch, D.A. Stoffers, E.J. Bernhard, and A.K. Rustgi. 2004. Successful growth and characterization of mouse pancreatic ductal cells: functional properties of the Ki-RAS(G12V) oncogene. *Gastroenterology.* 127:250–260. http://dx.doi.org/10.1053/j.gastro.2004.03.058

Sfondrini, L., A. Rossini, D. Besusso, A. Merlo, E. Tagliabue, S. Mènard, and A. Balsari. 2006. Antitumor activity of the TLR-5 ligand flagellin in mouse models of cancer. *J. Immunol.* 176:6624–6630. http://dx.doi.org/10.4049/jimmunol.176.11.6624

Spaner, D.E., and A. Masellis. 2007. Toll-like receptor agonists in the treatment of chronic lymphocytic leukemia. *Leukemia.* 21:53–60. http://dx.doi.org/10.1038/sj.leu.2404456

Surh, Y.J., A.M. Bode, and Z. Dong. 2010. Breaking the NF-κB and STAT3 alliance inhibits inflammation and pancreatic tumorigenesis. *Cancer Prev. Res.* 3:1379–1381. http://dx.doi.org/10.1158/1940-6207.CAPR-10-0251

Takeda, K., and S. Akira. 2007. Toll-like receptors. *Curr. Protoc. Immunol.* 77:14.12.1–14.12.13. http://dx.doi.org/10.1002/0471142735.im1412s77

Takeuchi, O., and S. Akira. 2010. Pattern recognition receptors and inflammation. *Cell.* 140:805–820. http://dx.doi.org/10.1016/j.cell.2010.01.022

Tan, M.C., P.S. Goedegebuure, B.A. Belt, B. Flaherty, N. Sankpal, W.E. Gillanders, T.J. Eberlein, C.S. Hsieh, and D.C. Linehan. 2009. Disruption of CCR5-dependent homing of regulatory T cells inhibits tumor growth in a murine model of pancreatic cancer. *J. Immunol.* 182:1746–1755. http://dx.doi.org/10.4049/jimmunol.182.3.1746

Tuomela, J., J. Sandholm, M. Kaakinen, A. Patel, J.H. Kauppila, J. Ilvesaro, D. Chen, K.W. Harris, D. Graves, and K.S. Selander. 2013. DNA from dead cancer cells induces TLR9-mediated invasion and inflammation in living cancer cells. *Breast Cancer Res. Treat.* 142:477–487. http://dx.doi.org/10.1007/s10549-013-2762-0

Volat, F.E., J.C. Pointud, E. Pastel, B. Morio, B. Sion, G. Hamard, M. Guichardant, R. Colas, A.M. Lefrançois-Martinez, and A. Martinez. 2012. Depressed levels of prostaglandin F2α in mice lacking Akr1b7 increase basal adiposity and predispose to diet-induced obesity. *Diabetes.* 61:2796–2806. http://dx.doi.org/10.2337/db11-1297

Vonlaufen, A., S. Joshi, C. Qu, P.A. Phillips, Z. Xu, N.R. Parker, C.S. Toi, R.C. Pirola, J.S. Wilson, D. Goldstein, and M.V. Apte. 2008. Pancreatic stellate cells: partners in crime with pancreatic cancer cells. *Cancer Res.* 68:2085–2093. http://dx.doi.org/10.1158/0008-5472.CAN-07-2477

Vonlaufen, A., P.A. Phillips, L. Yang, Z. Xu, E. Fiala-Beer, X. Zhang, R.C. Pirola, J.S. Wilson, and M.V. Apte. 2010. Isolation of quiescent human pancreatic stellate cells: a promising in vitro tool for studies of human pancreatic stellate cell biology. *Pancreatology.* 10:434–443. http://dx.doi.org/10.1159/000260900

Xu, H., H. An, Y. Yu, M. Zhang, R. Qi, and X. Cao. 2003. Ras participates in CpG oligodeoxynucleotide signaling through association with toll-like receptor 9 and promotion of interleukin-1 receptor-associated kinase/tumor necrosis factor receptor-associated factor 6 complex formation in macrophages. *J. Biol. Chem.* 278:36334–36340. http://dx.doi.org/10.1074/jbc.M305698200

Yadav, D., and A.B. Lowenfels. 2013. The epidemiology of pancreatitis and pancreatic cancer. *Gastroenterology.* 144:1252–1261. http://dx.doi.org/10.1053/j.gastro.2013.01.068

Yanai, H., T. Ban, and T. Taniguchi. 2012. High-mobility group box family of proteins: ligand and sensor for innate immunity. *Trends Immunol.* 33:633–640. http://dx.doi.org/10.1016/j.it.2012.10.005

Zambirinis, C.P., S. Pushalkar, D. Saxena, and G. Miller. 2014. Pancreatic cancer, inflammation, and microbiome. *Cancer J.* 20:195–202. http://dx.doi.org/10.1097/PPO.0000000000000045

Zheng, L., J. Xue, E.M. Jaffee, and A. Habtezion. 2013. Role of immune cells and immune-based therapies in pancreatitis and pancreatic ductal adenocarcinoma. *Gastroenterology.* 144:1230–1240. http://dx.doi.org/10.1053/j.gastro.2012.12.042

Zhu, F., P. Liu, J. Li, and Y. Zhang. 2014. Eotaxin-1 promotes prostate cancer cell invasion via activation of the CCR3-ERK pathway and upregulation of MMP-3 expression. *Oncol. Rep.* 31:2049–2054. http://dx.doi.org/10.3892/or.2014.3060